

# Transfer $Q^*$ : Principled Decoding for LLM Alignment

Souradip Chakraborty<sup>\*1</sup>, Soumya Suvra Ghosal<sup>\*1</sup>, Ming Yin<sup>2</sup>, Dinesh Manocha<sup>1</sup>,  
Mengdi Wang<sup>2</sup>, Amrit Singh Bedi<sup>†3</sup>, and Furong Huang<sup>†1</sup>

<sup>1</sup>University of Maryland, College Park

<sup>2</sup>Princeton University

<sup>3</sup>University of Central Florida

## Abstract

Aligning foundation models is essential for their safe and trustworthy deployment. However, traditional fine-tuning methods are computationally intensive and require updating billions of model parameters. A promising alternative, alignment via decoding, adjusts the response distribution directly without model updates to maximize a target reward  $r$ , thus providing a lightweight and adaptable framework for alignment. However, principled decoding methods rely on oracle access to an optimal Q-function ( $Q^*$ ), *which is often unavailable in practice*. Hence, prior SoTA methods either approximate this  $Q^*$  using  $Q^{\pi_{\text{sft}}}$  (derived from the reference SFT model) or rely on short-term rewards, resulting in sub-optimal decoding performance. In this work, we propose Transfer  $Q^*$ , which implicitly estimates the optimal value function for a target reward  $r$  through a baseline model  $\rho_{\text{BL}}$  aligned with a baseline reward  $r_{\text{BL}}$  (which can be different from the target reward  $r$ ). Theoretical analyses of Transfer  $Q^*$  provide a rigorous characterization of its optimality, deriving an upper bound on the sub-optimality gap and identifying a hyperparameter to control the deviation from the pre-trained reference SFT model based on user needs. Our approach significantly reduces the sub-optimality gap observed in prior SoTA methods and demonstrates superior empirical performance across key metrics such as coherence, diversity, and quality in extensive tests on several synthetic and real datasets.

## 1 Introduction

As artificial intelligence (AI) systems continue to demonstrate super-human performance across various tasks, it is becoming increasingly critical to ensure that such AI systems align well with human preferences, goals, and ethical standards. Alignment via fine-tuning with reinforcement learning from human feedback (RLHF) [38, 34, 9], has proven highly effective [36, 44]. However, aligning LLMs by fine-tuning the model parameters requires gradient updates across several billion

---

<sup>\*</sup>denotes equal contribution.

Emails: {schkra3, sghosal, dmanocha, furongh}@umd.edu, {my0049, mengdiw}@princeton.edu, {amritbedi@ucf.edu}.

<sup>†</sup>denotes equal contribution.

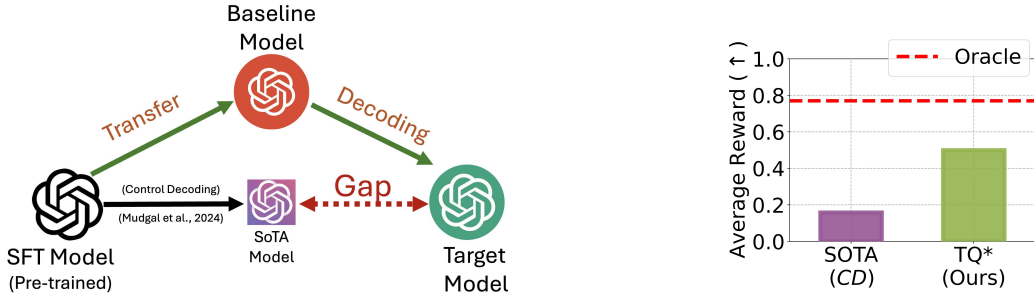


Figure 1: **Left.** This figure highlights the conceptual idea of proposed *transfer decoding* in this work. It clearly shows that the current SoTA method [33] exhibits suboptimality with respect to alignment with the target reward denoted by the dotted red arrow. On the other hand, the proposed transfer decoding method utilizes an immediately available aligned language model called the baseline, which is aligned with some baseline reward  $r_{BL}$  to bridge the gap between the SoTA method and the target model. **Right.** This figure provides empirical evidence of the performance gap of the current SoTA decoding strategy [33] with respect to Oracle (best of  $N$  sampling). Our proposed Transfer  $Q^*$  (TQ\*) reduces the gap and provides a new decoding method.

parameters (size of LLMs) which require vast computational resources [31, 25] and have a significant environmental impact [15]. Additionally, many SoTA models are not fully open-sourced [44, 36], offering limited access only to certain components like logits, making fine-tuning impossible.

As an alternative to fine-tuning, decoding for alignment has recently emerged as a potential solution [33, 26]. Decoding aims to alter the LLM’s response distribution at the token level to align with target reward  $r$  without updating the parameters of the LLM. Decoding facilitates alignment by accessing the token-level optimal value function,  $Q^*$ , which corresponds to the target reward  $r$ . Tokens are then sampled based on  $Q^*$ . This approach ensures rapid, efficient, and cost-effective alignment. A detailed discussion of related work is provided in Appendix C.

**A fundamental challenge.** Decoding effectively hinges on accessing an oracle to the optimal value function,  $Q^*$ , or a token-level optimal policy, which are typically not available in practical scenarios. To address this fundamental challenge, recent studies [33] have adopted a proxy,  $Q^{\pi_{sft}}$ , for  $Q^*$ . However, this approach results in suboptimal decoding due to a distribution shift inherent in approximating the true, unknown Q-function,  $Q^*$ , as illustrated in Figure 1. This raises a critical question:

*Is it possible to devise a more efficient and accurate estimate of the optimal value function  $Q^*$  for decoding purposes?*

In this work, we affirmatively address this query.

**Our approach** leverages a crucial observation regarding the key challenges identified: effective decoding requires access to a language model already aligned with the target reward  $r$  for trajectory-level response generation. Notably, recent advances in DPO-based methods [38, 3, 32] have facilitated the development of fine-tuned language models—referred to as baseline models—that are capable of generating aligned trajectories [27]. **Our first key idea** involves utilizing these publicly available trajectory-level models to estimate  $Q^*$  and subsequently derive the optimal token-level language model for decoding. We term this approach *direct transfer decoding*.

Moreover, it is possible that these publicly available baseline models are aligned with a different baseline reward  $r_{\text{BL}}$ , rather than the intended target reward  $r$ . **Our second key idea** addresses this challenge by proposing a novel *indirect transfer* decoding method. We introduce our proposed technique as Transfer Q\* (TQ\*), which facilitates efficient and on-the-fly alignment through decoding. We note that Transfer Q\* proves effective even when there are substantial discrepancies between the target and baseline rewards.

We summarize our **major contributions** as follows.

- **A novel concept of transfer decoding (TQ\*).** We introduce a novel concept of *transfer decoding* in a principled manner by leveraging already-available baseline language models aligned either with the target reward (direct transfer) or with some other (significantly) different baseline reward (indirect transfer). Our proposed approach TQ\* efficiently reduces the sub-optimality gap inherent in previous SoTA decoding methods, as highlighted in Figure 1.
- **Theoretical characterization of TQ\*.** We provide a rigorous theoretical characterization of the optimality of Transfer Q\*. Specifically, we derive an upper bound on the gap between the optimal LLM policy and the LLM decoding policy resulting from TQ\* (see Theorem 1). Additionally, we present a principled approach to control the deviation of the resulting policy from the pre-trained SFT language model  $\pi_{\text{sft}}$  (see Theorem 1, statement 2). This identifies hyperparameters that allow users to specify the desired amount of deviation or improvement based on their specific needs.
- **Experimental evaluations.** We provide a detailed empirical evaluation of TQ\* in various decoding tasks in both real and simulated settings, comparing against SoTA baselines, including DPO [38], ARGs [26], and CD [33]. Empirical results demonstrate consistent superiority over the baselines. Notably, TQ\* surpasses the current SoTA decoding strategy CD [33], achieving an improvement of up to 1.45x in average reward and 67.34% in GPT-4 based win-tie rate. We further evaluate and compare several attributes of the text generated by our algorithm (such as coherence, diversity, and quality) against baselines, demonstrating the superiority of our algorithm in all these aspects.

## 2 Problem Formulation: Alignment via Controlled Decoding

### 2.1 Token-level Markov Decision Process

Since the control decoding procedure operates at the token level, before formulating the problem mathematically, we start by defining a token-level Markov decision process (MDP) in the context of LLMs. Let us consider a token-level MDP  $\mathcal{M} := \{\mathcal{S}, \mathcal{A}, P, R\}$  with the state-space  $\mathcal{S}$  consisting of the concatenated sequence of tokens and the action space  $\mathcal{A}$  representing the space of the next token which is essentially the vocabulary  $\mathcal{V}$ .

**Next-token generator: the token-level policy  $\pi$ .** Given a state  $\mathbf{s}_t = [\mathbf{x}, \mathbf{y}_{<t}] \in \mathcal{S}$ , which is a sequence of tokens containing the prompt/query  $\mathbf{x} := \{x_1, x_2, \dots, x_N\}$  appended with the  $t$  tokens  $\mathbf{y}_{<t} := \{y_0, y_1, \dots, y_{t-1}\}$  generated so far, an LLM is a token-level decoding policy  $\pi$  that generates the action (i.e., the next token)  $a_t = y_t$  via sampling  $y_t \sim \pi(\cdot | \mathbf{s}_t)$ . The transition  $P$  to the next state  $\mathbf{s}_{t+1}$  is deterministic:  $\mathbf{s}_{t+1} = [\mathbf{x}, \mathbf{y}_{<t}, y_t]$ , the concatenation of the current state and action.

### Example 0: An instance of generated text responses of different decoding strategies

**Prompt:** How can I convert the decimal number 31 to binary format using JavaScript code? Can you provide the code for this conversion?

**ARGS:** Generate according to: 1. Convert decimal number 31 to binary format. 2. Convert binary number 10110 to decimal format. 3. Convert octal number 37 to decimal format. 4. Convert hexadecimal number A5 to decimal format. 5. Convert decimal number 100 to binary format. 6. Convert decimal number 1100100 to binary format. 7. Convert decimal number 255 to binary format. 8. Convert decimal number 101001001001

**CD<sup>-</sup>:** To convert a decimal number to binary format using JavaScript, you can use the bitwise right shift operator ('>') to divide the decimal number by 2 repeatedly until the result is 0. The binary digits (bits) are obtained by checking the remainder of each division. Here's the JavaScript code to convert decimal number 31 to binary format:

```
let decimal = 31;
let binary = "";
while (decimal > 0) let remainder = decimal % 2;
binary = remainder + binary;
```

**TQ\* (Ours):** To convert a decimal number to binary format using JavaScript, you can use the 'toString(2)' method. This method converts a number to a string representation with base 2 (binary). Here's the code to convert decimal number 31 to binary format using JavaScript:

```
let decimalNumber = 31;
let binaryNumber = decimalNumber.toString(2);
console.log(binaryNumber);
Output: '11111'
```

**Response generator: the trajectory-level policy  $\rho$ .** We denote the trajectory level probability by  $\rho_\pi(\mathbf{y}|\mathbf{x}) = \prod_{t=1}^T \pi(y_t|[\mathbf{x}, \mathbf{y}_{<t}])$ . Some commonly used sampling techniques in the literature include Beam Search [17], Top-p sampling [20], and Top-k Sampling [16].

**From trajectory-level reward  $r$  to token-level reward  $R$ .** Successful decoding depends on sampling from a token-level policy that yields high rewards, reflecting the inherently token-level nature of the decoding process. However, as detailed in Appendix D, we obtain a reward model  $r(\mathbf{x}, \mathbf{y})$ , only at the trajectory-level rather than the desired token-level, by fitting feedback on human preferences. To close the gap, similar to existing literature [33], we define the token-level reward  $R(\mathbf{x}, y_t)$  from the trajectory-level reward model  $r(\mathbf{x}, \mathbf{y})$  as follows:

$$R(\mathbf{x}, y_t) := \begin{cases} 0, & y_t \neq \text{EOS} \\ r(\mathbf{x}, \mathbf{y}_{<t}), & y_t = \text{EOS}, \end{cases} \quad (1)$$

where  $\text{EOS} \in \mathcal{V}$  represents the end of sequence token. The token-level reward in (1) implies that we only receive a reward once we have the full sequence/response, otherwise, no reward.

**Action-value function  $Q^\pi$  for  $\pi$  and optimal  $Q^*$  for optimal  $\pi^*$ .** From the token-level reward



$R(\mathbf{x}, y_t)$ , we can define the action-value function associated with the reward as

$$Q^\pi(\mathbf{s}_t, a_t) = Q^\pi([\mathbf{x}, \mathbf{y}_{<t}], y_t) = \mathbb{E} \left[ \sum_i R([\mathbf{x}, \mathbf{y}_{<t}], z_i) \mid z_0 = y_t, z_i \sim \pi(\cdot | \mathbf{s}_{t+i}) \right], \quad (2)$$

where  $\mathbf{s}_{t+i} := [\mathbf{s}_t, z_0, z_1, \dots, z_{i-1}]$  and expectation is over the randomness due to the sampling from token level language model  $\pi$ . The optimal Q-function from the definition in equation (2) is given by

$$Q^*(\mathbf{s}_t, a_t) = \max_{\pi} Q^\pi(\mathbf{s}_t, a_t). \quad (3)$$

The optimization problem in (3) denotes an unconstrained objective as in standard reinforcement learning; however, in the context of alignment for LLMs, we also need to consider the distance of optimal aligned policy to the pre-trained unaligned token-level policy  $\pi_{\text{sft}}$  [37, 41, 38].

## 2.2 Principled Decoding for LLM Alignment

In this section, we will formulate the problem of aligning LLMs during deployment via a controlled decoding procedure as initially discussed in [33, 26].

**Decoding process.** We start by defining what decoding means in the context of LLMs. We consider access to a pre-trained unaligned language model  $\pi_{\text{sft}}$  which takes in prompt  $\mathbf{x}$  as an input and generates a response  $\mathbf{y} = [y_0, y_1, \dots, \text{EOS}]$  token by token by sampling  $y_t \sim \pi_{\text{sft}}(\cdot | [\mathbf{x}, \mathbf{y}_{\leq t}])$  for all  $t$ . This token-by-token generation of response is called decoding in LLMs. Hence, the natural next question arises if we can control the decoding process and generate responses that are aligned with respect to a target reward function  $r(\mathbf{x}, \mathbf{y})$ . The quest to answer this question has given rise to an interesting research problem of utilizing decoding for LLM alignment [33].

**LLM alignment via decoding.** The problem of LLM alignment via decoding can be formally defined as solving for the optimal decoding policy  $\pi_{\text{dec}}^*$  under the token level MDP  $\mathcal{M}$  as

$$\pi_{\text{dec}}^*(\cdot | \mathbf{s}_t) := \arg \max_{\pi \in \Pi} \mathbb{E}_{z \sim \pi(\cdot | \mathbf{s}_t)} [Q^*(\mathbf{s}_t, z)] - \alpha \mathbb{D}_{\text{KL}} [\pi(\cdot | \mathbf{s}_t) || \pi_{\text{sft}}(\cdot | \mathbf{s}_t)], \quad (4)$$

where  $\mathbf{s}_t = [\mathbf{x}, \mathbf{y}_{<t}]$  and  $Q^*(\mathbf{s}_t, z)$  denotes the optimal state-action value function for the token-level MDP  $\mathcal{M}$  defined in (3). We remark that the KL regularization in equation (4) ensures that the optimal decoding policy  $\pi_{\text{dec}}^*$  remains in the close neighborhood of the pre-trained model  $\pi_{\text{sft}}$  which contains other important properties. In (4),  $\alpha > 0$  denotes the alignment hyperparameter which controls the trade-off between the objective of maximizing the target reward  $r$  return and the closeness to  $\pi_{\text{sft}}$ . We can write the closed-form solution of the problem in (4) as

$$\pi_{\text{dec}}^*(z | \mathbf{s}_t) = \pi_{\text{sft}}(z | \mathbf{s}_t) \frac{\exp(\frac{1}{\alpha} Q^*(\mathbf{s}_t, z))}{C_\alpha}, \quad (5)$$

where  $C_\alpha := \sum_z \pi_{\text{sft}}(z | \mathbf{s}_t) \exp(\alpha Q^*(\mathbf{s}_t, z))$  is the normalizing constant for state  $\mathbf{s}_t$ . Although the close form expression in (5) poses an interesting form, it is difficult to implement it in practice due to the various challenges we will discuss next.

**Challenges of implementing (5): oracle access to the optimal  $Q^*$ .** A major challenge in implementing the aligned decoding policy in (5), lies in the requirement of access to the optimal  $Q^*(\mathbf{s}_t, z)$

in (5) for each state-action pair  $(s_t, z)$ , which is unavailable in practice. To emphasize that, first we note that  $Q^*(s_t, z)$  in (3) can be written using the trajectory level reward  $r$  as

$$Q^*(s_t, z) = \mathbb{E}_{\tau \sim \rho^*(\cdot|s_t, z)} [r(\mathbf{x}, \mathbf{y}_{<t}, z, \tau)], \quad (6)$$

where  $\tau$  denotes the trajectory  $\tau := \{z_1, z_2, \dots, z_T\}$ , and  $\rho^*(\cdot|s_t, z) = \prod_{i=1}^T \pi^*(z_i|[s_{t+i}])$  represents the distribution over the trajectory level response induced by the optimal policy  $\pi^*(\cdot|s_t)$  (cf. (3)). From (6), we note that the optimal  $Q^*(s_t, z)$  relies on the trajectory/response generated by the optimal  $\rho^*$  which is unknown. This creates a bottleneck in efficiently deploying the decoding policy in (5) for alignment with target reward  $r$ . Next, we discuss how some existing approaches in the literature deal with this fundamental issue and what the limitations are.

**Limitations in existing approaches.** An interesting approach called *controlled decoding (CD)* is proposed in recent literature by Mudgal et al. [33], and it approximates  $Q^*(s_t, z)$  by  $Q^{\pi_{\text{sft}}}(s_t, z)$ , which is tractable and easily computable due to availability of  $\pi_{\text{sft}}$ . However, this approximation results in significant suboptimal performance, as described in Figure 1 (right). Given this limitation of existing approaches and the above-mentioned fundamental challenge of decoding, we pose the question: Is it possible to provide a better estimate of  $Q^*$  for decoding? We answer this affirmatively in the following section by introducing a novel concept of *transfer decoding*.

### 3 Proposed Approaches: Alignment via Transfer $Q^*$

**Our key ideas of transfer decoding.** Our proposed approach hinges on an interesting observation that recent advancements in alignment, particularly through direct preference optimization (DPO)-based approaches [38], have led to the development of open source freely available fine-tuned language models [27, 53]. We call such aligned models as baseline models, that generate trajectory responses in an aligned manner. **Our first key idea** is to utilize these baseline models aligned with target reward  $r$ , if available, to estimate  $Q^*$  and subsequently derive the optimal token-level language model for decoding. We remark that baseline models are aligned at the trajectory level (see Appendix D for details), while decoding requires the optimal models at the token level. We term this approach *direct transfer decoding*. However, it is possible that the available aligned baseline model is aligned with a different baseline reward  $r_{\text{BL}}$  instead of the target reward  $r$ . Hence, **our second key idea** addresses this issue by proposing a novel method called *indirect transfer decoding*. We discuss both the ideas and detailed algorithms in detail next.

#### 3.1 Direct Transfer Decoding

For the direct transfer, we start by considering that we are given a target reward model  $r$  and an unaligned pre-trained SFT language model given by  $\pi_{\text{sft}}$ ; the corresponding trajectory-level response distribution is given by  $\rho_{\text{sft}}$ . We are operating under the assumption that we have a baseline model  $\rho_{\text{BL}}(\mathbf{y}|\mathbf{x})$  with target reward  $r$ . We note that the closed-form expression for the RLHF-aligned optimal model  $\rho_{\text{BL}}$  can be written as (see Appendix D, Equation (25)) follows:

$$\rho_{\text{BL}}(\mathbf{y}|\mathbf{x}) = \frac{1}{Z_r(\mathbf{x})} \rho_{\text{sft}}(\mathbf{y}|\mathbf{x}) \exp\left(\frac{1}{\beta} r(\mathbf{x}, \mathbf{y})\right), \quad (7)$$

where  $Z_r(\mathbf{x})$  is the normalizing constant and  $\beta > 0$  is the trajectory-level alignment parameter. We note that the trajectory level optimal policy in (7) is usually obtained in the literature via the fine-tuning stage and efficient algorithms such as DPO [38].

**Estimating  $Q^*$  for direct transfer.** Now we get back to the fundamental bottleneck of optimal decoding, which lies in estimating the token-level optimal  $Q^*(\mathbf{s}_t, z)$ . We propose providing a solution to the problem with the help of  $\rho_{\text{BL}}(\mathbf{y}|\mathbf{x})$ . As defined in (6), we begin by considering

$$Q^*(\mathbf{s}_t, z) = \mathbb{E}_{\tau \sim \rho^*(\cdot|\mathbf{s}_t, z)} [r([\mathbf{s}_t, z], \tau)], \quad (8)$$

where  $\rho^*(\cdot|\mathbf{s}_t, z) := \arg \max_{\rho} \mathbb{E}_{\tau \sim \rho(\cdot|\mathbf{s}_t, z)} [r(\mathbf{s}_t, \tau)]$ . However, we know that the available baseline model  $\rho_{\text{BL}}(\mathbf{y}|\mathbf{x})$  in (7) is the solution of following optimization problem:

$$\rho_{\text{BL}}(\cdot|\mathbf{x}) := \arg \max_{\rho} \mathbb{E}_{\tau \sim \rho(\cdot|\mathbf{x})} [r(\mathbf{x}, \tau)] - \beta \mathbb{D}_{\text{KL}}[\rho(\cdot|\mathbf{x}) \parallel \rho_{\text{sft}}(\cdot|\mathbf{x})], \quad (9)$$

which constraints the drift of the optimal distribution  $\rho_{\text{BL}}$  from the trajectory level reference policy  $\rho_{\text{sft}}$  with the KL divergence term. We propose approximating the optimal  $Q^*(\mathbf{s}_t, z)$  for decoding by

$$\text{TQ}^*(\mathbf{s}_t, z) = \mathbb{E}_{\tau \sim \rho_{\text{BL}}(\cdot|\mathbf{s}_t, z)} [r([\mathbf{s}_t, z], \tau)]. \quad (10)$$

With the definition in (10), we propose obtaining our token-level decoding policy  $\pi_{\text{Alg}}^*(\cdot|\mathbf{s}_t)$  for the token-level MDP as

$$\pi_{\text{Alg}}^*(\cdot|\mathbf{s}_t) := \arg \max_{\pi \in \Pi} \mathbb{E}_{z \sim \pi(\cdot|\mathbf{s}_t)} [\text{TQ}^*(\mathbf{s}_t, z)] - \alpha \mathbb{D}_{\text{KL}}[\pi(\cdot|\mathbf{s}_t) \parallel \pi_{\text{BL}}(\cdot|\mathbf{s}_t)], \quad (11)$$

where  $\pi_{\text{BL}}(\cdot|\mathbf{s}_t)$  is the token-level language model, which induces the trajectory level model  $\rho_{\text{BL}}$ . Due to the strong convexity of the objective in (11) owing to the additional KL regularization term, we get the closed-form solution of  $\pi_{\text{Alg}}^*(\cdot|\mathbf{s}_t)$  as

$$\pi_{\text{Alg}}^*(z|\mathbf{s}_t) = \frac{1}{\tilde{C}_{\alpha}(\mathbf{s}_t)} \pi_{\text{BL}}(z|\mathbf{s}_t) \exp\left(\frac{1}{\alpha} \cdot \text{TQ}^*(\mathbf{s}_t, z)\right), \quad (12)$$

where  $\tilde{C}_{\alpha}(\mathbf{s}_t)$  is the normalizing constant. We summarize the proposed approach in Algorithm 1.

## 3.2 Indirect Transfer Decoding

We remark that, for the direct transfer decoding, we started with the assumption that the available baseline model  $\rho_{\text{BL}}$  is aligned with the target model only. In practice, however, it is possible that the freely available baseline model  $\rho_{\text{BL}}$  is actually aligned with some other reward function we call baseline  $r_{\text{BL}}$  rather than the target reward  $r$ . We argue that this condition is even more easily satisfied under the ongoing active research scenario in alignment because we have easy access to open-source, well-aligned LLMs trained on various reward functions [27, 52, 13, 38]. Under this setting of baseline reward  $r_{\text{BL}}$  and language model  $\rho_{\text{BL}}$ , we define our novel indirect transfer decoding process as follows.

---

**Algorithm 1** Transfer  $Q^*$ : LLM Alignment via Transfer Decoding
 

---

- 1: **Input:** Trajectory level baseline model  $\rho_{\text{BL}}(\mathbf{y}|\mathbf{x})$  aligned with baseline reward  $r_{\text{BL}}$ , target reward  $r$ , token-level baseline policy  $\pi_{\text{BL}}$ , number of tokens sampled  $k$ , decoding alignment parameter  $\alpha$ , vocabulary set  $\mathcal{V}$ .
  - 2: **for**  $t = 0, \dots, T$  **do**
  - 3:     Current state :  $\mathbf{s}_t = [\mathbf{x}, \mathbf{y}_{<t}]$ , where  $\mathbf{x}$  is prompt and  $\mathbf{y}_{<t} = [y_0, y_1, \dots, y_{t-1}]$
  - 4:     Sample top-k tokens using token-level baseline policy  $\pi_{\text{BL}}$  and store as  $\hat{\mathcal{V}} = \{z_i : z_i \sim \pi_{\text{BL}}(\cdot|\mathbf{s}_t)\}_{i=1}^k$ .
  - 5:     **for**  $z \in \hat{\mathcal{V}}$  **do**
  - 6:         **if**  $r_{\text{BL}} = r$  **then** (Direct transfer)
  - 7:             **Evaluate**  $\text{TQ}^*(\mathbf{s}_t, z) = r([\mathbf{s}_t, z], \tau)$ , where  $\tau \sim \rho_{\text{BL}}(\cdot|[\mathbf{s}_t, z])$
  - 8:         **else** (Indirect transfer)
  - 9:             **Evaluate**  $\text{TQ}^*(\mathbf{s}_t, z) = w \cdot r([\mathbf{s}_t, z], \tau)$  where  $\tau \sim \rho_{\text{BL}}(\cdot|[\mathbf{s}_t, z])$ ,  $w = \frac{\rho_r(\tau|[\mathbf{s}_t, z])}{\rho_{\text{BL}}(\tau|[\mathbf{s}_t, z])}$
  - 10:         **Estimate** decoding probability  $\pi_{\text{Alg}}^*(z|\mathbf{s}_t) \propto \pi_{\text{BL}}(z|\mathbf{s}_t) \exp\left(\frac{1}{\alpha} \cdot \text{TQ}^*(\mathbf{s}_t, z)\right)$
  - 11:     **Next token**  $y_t \sim \pi_{\text{Alg}}^*(\cdot|\mathbf{s}_t)$
  - 12:     **Next state**  $\mathbf{s}_{t+1} \leftarrow [\mathbf{s}_t, y_t]$
  - 13: **Return**  $\mathbf{y} = [y_0, \dots, y_T]$
- 

**The Transfer Process.** The baseline language model  $\rho_{\text{BL}}$  is also an RLHF aligned model corresponding to reward function  $r_{\text{BL}}$ . It holds that:

$$r_{\text{BL}}(\mathbf{x}, \mathbf{y}) = \beta \log \frac{\rho_{\text{BL}}(\mathbf{y}|\mathbf{x})}{\rho_{\text{sft}}(\mathbf{y}|\mathbf{x})} + \beta \log Z_{\text{BL}}(\mathbf{x}). \quad (13)$$

where  $Z_{\text{BL}}(\mathbf{x})$  is the corresponding partition function. From the closed-form expression in (7), it holds for the target reward  $r$  that

$$r(\mathbf{x}, \mathbf{y}) = \beta \log \frac{\rho_r(\mathbf{y}|\mathbf{x})}{\rho_{\text{sft}}(\mathbf{y}|\mathbf{x})} + \beta \log Z_r(\mathbf{x}). \quad (14)$$

Using equations (14) and (13), we can obtain the trajectory-level optimal policy  $\rho_r(\mathbf{y}|\mathbf{x})$  for the target reward  $r(\mathbf{x}, \mathbf{y})$  as :

$$\rho_r(\mathbf{y}|\mathbf{x}) = \underbrace{\rho_{\text{BL}}(\mathbf{y}|\mathbf{x}) \exp\left[\frac{1}{\beta}(r(\mathbf{x}, \mathbf{y}) - r_{\text{BL}}(\mathbf{x}, \mathbf{y}))\right]}_{:=\tilde{\rho}_r(\mathbf{y}|\mathbf{x})} \frac{Z_{\text{BL}}(\mathbf{x})}{Z_r(\mathbf{x})}, \quad (15)$$

where we note that  $\tilde{\rho}_r(\mathbf{y}|\mathbf{x})$  is the unnormalized probability with the normalization factory  $\tilde{Z}(\mathbf{x}) := \frac{Z_r(\mathbf{x})}{Z_{\text{BL}}(\mathbf{x})}$ . We show in the Appendix F that  $\tilde{Z}(\mathbf{x})$  is the normalization constant for  $\tilde{\rho}_r(\mathbf{y}|\mathbf{x})$ . We emphasize that calculating the trajectory-level optimal language model for the target reward function  $r$  in (15) is the crucial step in estimating the optimal  $Q^*$  for the token-level MDP  $\mathcal{M}$  for our decoding.

**Estimating  $Q^*$  for indirect transfer.** Similar to the direct transfer setting, we propose approximat-

ing the optimal  $Q^*(\mathbf{s}_t, z)$  for decoding by using  $\rho_r(\mathbf{y}|\mathbf{x})$  in (15) as

$$\begin{aligned} \text{TQ}^*(\mathbf{s}_t, z) &= \mathbb{E}_{\tau \sim \rho_r(\cdot|\mathbf{s}_t, z)} [r([\mathbf{s}_t, z], \tau)]. \\ &= \mathbb{E}_{\tau \sim \rho_{\text{BL}}(\cdot|\mathbf{s}_t, z)} \left[ \frac{\rho_r(\mathbf{y}|\mathbf{x})}{\rho_{\text{BL}}(\mathbf{y}|\mathbf{x})} r([\mathbf{s}_t, z], \tau) \right] \end{aligned} \quad (16)$$

where we use the importance sampling trick and then utilizing equation (15), we can get the  $Q^*$  for indirect transfer. Now, following (11) and (12), we can write

$$\pi_{\text{Alg}}^*(\cdot|\mathbf{s}_t) := \arg \max_{\pi \in \Pi} \mathbb{E}_{z \sim \pi(\cdot|\mathbf{s}_t)} [\text{TQ}^*(\mathbf{s}_t, z)] - \alpha \mathbb{D}_{\text{KL}}[\pi(\cdot|\mathbf{s}_t) || \pi_r(\cdot|\mathbf{s}_t)], \quad (17)$$

where  $\pi_r(\cdot|\mathbf{s}_t)$  is the token level probability derived from the trajectory level policy  $\rho_r(\cdot|\mathbf{s}_t)$  in (15). Following (11) and (12), we can obtain our optimal decoding policy for the indirect transfer as well. We summarize the proposed approach in Algorithm 1.

### 3.3 Theoretical Results and Insights

This subsection provides the theoretical analysis of our Transfer  $Q^*$  algorithm under direct transfer setup. Existing works [33, 18] leverage the reward-KL tradeoff curve to measure the *reward gain* versus *deviation from reference policy*. Ideally, a good algorithm should achieve high rewards while staying close to the reference policy (be KL-efficient). We follow these two aspects and consider two performance metrics: (1) suboptimality gap and (2) KL divergence between our algorithm’s policy and the SFT policy. Specifically, we borrow the notion of a suboptimality-gap from offline RL literature [1] and define it in terms of value function difference for any prompt  $\mathbf{x}$  as

$$\text{Sub-Gap}(\mathbf{x}) := V^*(\mathbf{x}) - V_{\text{Alg}}(\mathbf{x}). \quad (18)$$

where  $V^*(\mathbf{x}) = \max_{\rho} \mathbb{E}_{\tau \sim \rho(\cdot|\mathbf{x})} [r(\mathbf{x}, \tau)]$ ,  $V_{\text{Alg}}(\mathbf{x}) = \mathbb{E}_{\tau \sim \rho_{\text{Alg}}^*(\cdot|\mathbf{x})} [r(\mathbf{x}, \tau)]$ , and  $\rho_{\text{Alg}}^*$  represents the distribution over the trajectories induced by the token level policy  $\pi_{\text{Alg}}^*(\cdot|\mathbf{x})$  in (17). The KL divergence between our algorithm and the reference policy is denoted by  $\mathbb{D}_{\text{KL}}(\rho_{\text{Alg}}^*(\cdot|\mathbf{x}), \rho_{\text{sft}}(\cdot|\mathbf{x}))$ . We present our main theorem as follows, and the full proof is deferred to Appendix E.

**Theorem 1.** *For the proposed Transfer  $Q^*$  Algorithm 1, the following results hold.*

(1) *Suboptimality gap for all  $\mathbf{x}$  is upper bounded as*

$$\text{Sub-Gap}(\mathbf{x}) \leq \beta \mathbb{D}_{\text{KL}}(\rho^*(\cdot|\mathbf{x}), \rho_{\text{sft}}(\cdot|\mathbf{x})) - \alpha h_{\alpha}(\mathbf{x}), \quad (19)$$

where  $\beta$  is defined in (9) for baseline policy, and  $\alpha$  is defined in (17) for decoding process. Here  $h_{\alpha}(\mathbf{x}) \geq 0$  and its formula is defined in Appendix E.

(2) *Assume reward satisfies  $0 \leq r \leq r_{\text{max}}$ . then the divergence to SFT policy is given by*

$$\mathbb{D}_{\text{KL}}(\rho_{\text{Alg}}^*(\cdot|\mathbf{x}), \rho_{\text{sft}}(\cdot|\mathbf{x})) \leq \left( \frac{1}{\beta} + \frac{1}{\alpha} T \right) r_{\text{max}}. \quad (20)$$

**Remark 1 (“Double Robustness” of Transfer  $Q^*$ ).** Theorem 1 indicates the suboptimality is bounded by  $\beta \mathbb{D}_{\text{KL}}(\rho^*, \rho_{\text{sft}})$ , and this guarantees our algorithm will achieve high accuracy in two cases. 1. The penalty parameter  $\beta$  is small, 2. The SFT policy  $\rho_{\text{sft}}$  is close to  $\rho^*$ . In addition, our decoding design (17) is also effective for improving the performance. This is due to  $-\alpha h_\alpha \leq 0$ . Our decoding coefficient  $\alpha$  could further reduce the suboptimality gap when it is appropriately tuned (e.g. choose  $\alpha^* = \arg \min_\alpha \alpha h_\alpha$ ).

**Remark 2 (KL-Efficiency of Transfer  $Q^*$ ).** Via Theorem 1, the deviation from our algorithm to the reference policy is jointly controlled by parameter  $\beta$  and decoding parameter  $\alpha$ . When both parameters are set large, our algorithm is more conservative and hence more KL-efficient. When the parameters are small, the KL deviation becomes larger.

## 4 Experimental Evaluations

We present a comprehensive empirical analysis of both direct and indirect Transfer  $Q^*$ , tested across various open-source datasets and state-of-the-art models [27]. Our findings demonstrate TQ $^*$ ’s effectiveness in aligning language model outputs with specific target rewards. For implementation, we set the number of tokens sampled  $k = 10$  and the decoding alignment parameter  $\alpha = 1$ . We report ablations in Appendix H.3. Reproducibility is ensured through the use of publicly available resources.

Table 1: Summary of the datasets and model architectures used for experimental evaluations in Section 4.1.

Dataset		Model Architectures			Reward Preference
		SFT	DPO	Reward	
Evaluation-1	UltraFeedback [12]	Mistral-7B- $\alpha$ [24]	Zephyr-7B- $\alpha$ [46]	Mistral-7B- $\alpha$ [24]	Relevant, Helpful, and Ethical responses.
Evaluation-2	HH-RLHF [5]	Pythia-6.9B [7]	Pythia-6.9B [7]	Pythia-6.9B [7]	Helpful and Harmless responses.
Evaluation-3	Berkeley Nectar [53]	OpenChat 3.5-7B [47]	Starling-7B- $\alpha$ [53]	Mistral-7B- $\alpha$ [24]	Accurate, Helpful, and Harmless responses.
Evaluation-4	UltraFeedback [12]	Llama-2-7B [45]	Tulu-v2-7B [23]	Mistral-7B- $\alpha$ [24]	Relevant, Helpful, and Ethical responses.
Evaluation-5	UltraFeedback [12]	Mistral-7B- $\alpha$ [24]	Zephyr-7B- $\alpha$ [46]	Gemma-7B [6]	Relevant, Helpful, and Ethical responses.
Evaluation-6	UltraFeedback [12]	Mistral-7B- $\alpha$ [24]	Zephyr-7B- $\alpha$ [46]	Gemma-2B [6]	Relevant, Helpful, and Ethical responses.

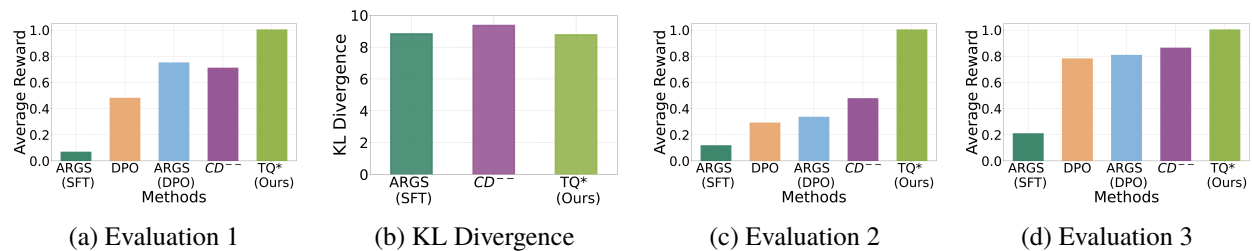


Figure 2: In plots (a), (c), and (d) we present the normalized average reward values obtained using the corresponding setup outlined in Table 1. ARGs (SFT) and ARGs (DPO) refer to the reward modeling approach described in [26] to the SFT and DPO model respectively. Our analysis reveals that across all setups, TQ $^*$  consistently outperforms other competitive baselines summarized in Table 1, demonstrating its superior efficacy. We report results on other evaluation setups in Appendix H. In (b), we compare (for Evaluation-1 setup) the trajectory-level KL Divergence between different decoding policies and the base model  $\rho_{\text{sft}}$  to show the effectiveness of the proposed approach compared to the state-of-the-art.



**Evaluation Methodology.** For evaluation, we compare the performance of the response generated by the language model corresponding to each prompt in the test dataset. Following [26], we limit the maximum length of the prompt and generated continuation to 128 and 2048 tokens, respectively. For all baselines, we utilize a greedy-based sampling method. The quality of the generated responses is assessed based on multiple attributes (including reward achieved, win-tie rate, coherence, diversity, etc.) using the following evaluation metrics [26]:

- **Average Reward:** We report the mean of the rewards for generations corresponding to all prompts in the test set. A higher mean reward score signifies that the model’s outputs are better aligned with the attributes represented in the reward model.
- **Diversity:** This metric measures the ability to generate texts with a wide range of vocabulary. Specifically, it calculates the frequency of repeated n-grams in text.
- **Coherence:** We assess the semantic closeness between each prompt and its generated response using the cosine similarity of their SimCSE-generated [43] embeddings.

## 4.1 Evaluations with Direct Transfer Decoding

**Experiment Details.** For the direct transfer experiments, we consider our baseline model as a DPO [38] fine-tuned model aligned with the target reward. To evaluate the performance of Transfer  $Q^*$  (denoted as  $TQ^*$  in figures), we conduct experiments across multiple datasets and model architectures, encompassing 6 distinct tasks. Our experimentation is primarily based on the Ultrafeedback [12], Berkeley Nectar [53], and HH-RLHF (Helpful and Harmless) [5] datasets. For each task, we utilize the DPO [38] fine-tuned model as an aligned policy, with configurations listed in Table 1. This comprehensive approach allows us to gauge the adaptability and efficacy of  $TQ^*$  in various contexts, providing a robust measure of its capabilities. **Results Discussion.** In

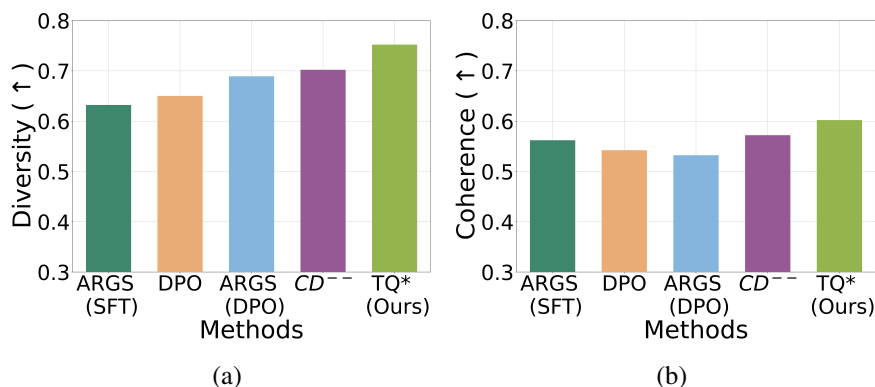


Figure 3: **Diversity and Coherence analysis of generated responses.** We observe that the responses generated using  $TQ^*$  obtain the highest coherence and diversity. These results are based on the prompts from the Berkeley Nectar dataset.

Figure 2, we present the normalized average rewards for the first three setups detailed in Table 1. We report the results for other setups in Appendix H.1. We compare our proposed method  $TQ^*$

with competitive existing approaches such as ARGES [26], CD<sup>−−</sup> [33]<sup>1</sup>, and DPO [38]. To provide a clearer comparison of results, we normalize the average rewards (further details of normalization in Appendix G.1). We observe that across all setups, TQ<sup>\*</sup> consistently outperforms the existing approaches by a large margin, highlighting its efficacy in learning token-level optimal policy during inference. Further, in Figure 3, we report that TQ<sup>\*</sup> not only produces responses with high rewards but also outperforms other decoding strategies in terms of diversity and coherence.

**GPT-4 Evaluation.** To further understand the quality of the responses generated, we employ a GPT-4-based evaluation framework. Specifically, we use GPT-4 as a surrogate for human assessment. In this method, we prompt GPT-4 to assess and rate two responses on the same prompt on a scale

Table 2: **GPT-4 Based Evaluation.** We prompt GPT-4 to rate responses from various decoding strategies on relevance, accuracy, and insightfulness, scoring them from 1 to 10. A higher win-tie percentage indicates our method’s effectiveness in generating contextually relevant and accurate responses.

Ours	vs.	Methods	Win-Tie (%) ↑		
			Evaluation-1	Evaluation-2	Evaluation-3
TQ <sup>*</sup>		ARGES-SFT	86.67	72.00	75.34
TQ <sup>*</sup>		DPO	70.67	77.34	70.00
TQ <sup>*</sup>		ARGES-DPO	68.00	71.33	74.00
TQ <sup>*</sup>		CD <sup>−−</sup>	66.67	65.34	67.34

from 1 to 10, focusing on criteria such as relevance, accuracy, and insightfulness. For this, we randomly sample 300 prompts from the test set and compare the response between TQ<sup>\*</sup> and other competitive decoding methods. We present the GPT-4 evaluation results in Table 2, measured by the percentage of win-ties of our method over the alternative decoding strategies. A higher percentage indicates that our proposed method is more proficient in generating responses that exhibit better alignment with human preferences. Our analysis in Table 2 shows that TQ<sup>\*</sup> consistently has a higher win-tie percentage compared to other decoding approaches, reaffirming its efficacy.

## 4.2 Evaluations with Indirect Transfer Decoding

**Synthetic experiments.** In the synthetic experiments, we simulate four scenarios to examine shifts in the reward distribution between source and target reward models. These scenarios are instrumental in elucidating the advantages of our proposed method. The shift in reward distribution is achieved through model intervention techniques, such as inducing sparsity in the final linear layer. Our analysis utilizes the UltraFeedback [12] and Berkeley Nectar [53] datasets. The specifics of the models utilized are detailed in Table 4 in Appendix G.2. For each dataset, we design two transfer tasks by modulating the reward distribution. We visualize the shift in reward distribution on the Ultrafeedback dataset in Figure 4 (a) and (c) respectively. Given that this is a synthetic setup, no DPO-aligned policies exist for the newly generated reward distribution, which underscores the significance of

<sup>1</sup>Due to unavailability of code base, we compare using an approximate version of CD [33] in which we do not train an adapter module.

addressing the transfer problem. We present the results for this analysis on the Ultrafeedback [12] dataset in Figure 4. Due to space constraints, we report the results on the Berkeley Nectar [53] in Appendix H.2. We make the following key observations: (1) Our proposed decoding framework consistently attains the highest average reward and outperforms other competitive strategies. (2) The variant of our decoding strategy obtained by direct transfer to the target reward, i.e., DT has subpar performance.

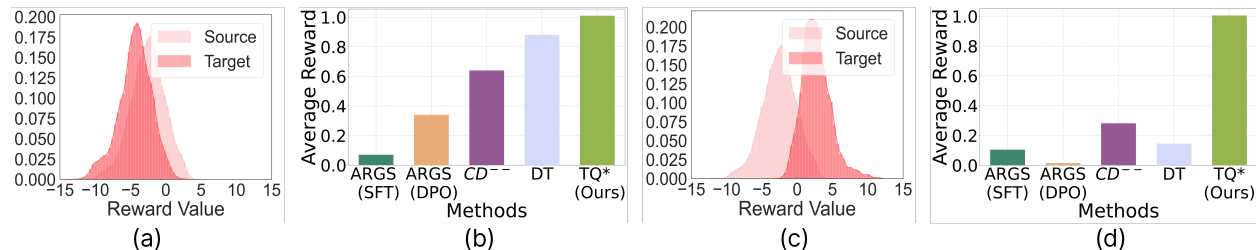


Figure 4: **Evaluation for Synthetic Indirect Transfer Tasks.** We plot the distribution of the reward values for the source and two transfer tasks on the Ultrafeedback in (a) and (c). The reward model architecture is Mistral-7B- $\alpha$  [24]. In (b) and (d), we compare the normalized average reward scores for competitive decoding strategies. We represent the variant of our decoding strategy with direct transfer as DT. We observe that TQ\* consistently outperforms the other baselines. Results on other datasets are reported in Appendix H.2.

**Real transfer experiments.** To further evaluate our proposed approach on real reward transfer, we consider two transfer setups as outlined in Table 5 in Appendix G.3. We illustrate the distribution shift in reward values on UltraFeedback [12] and HH-RLHF [5] datasets in Figure 5 (a) and (c) respectively. We compare the normalized average reward values of different decoding strategies in Figure 5. Consistent with our findings from the synthetic experiments, our proposed method consistently outperforms other decoding strategies, underscoring its effectiveness in real transfer tasks as well. Notably, we observe that even when there is a significant shift in the source and target reward values, as evident in Figure 5 (c), TQ\* outperforms all competitive decoding approaches in terms of average reward.

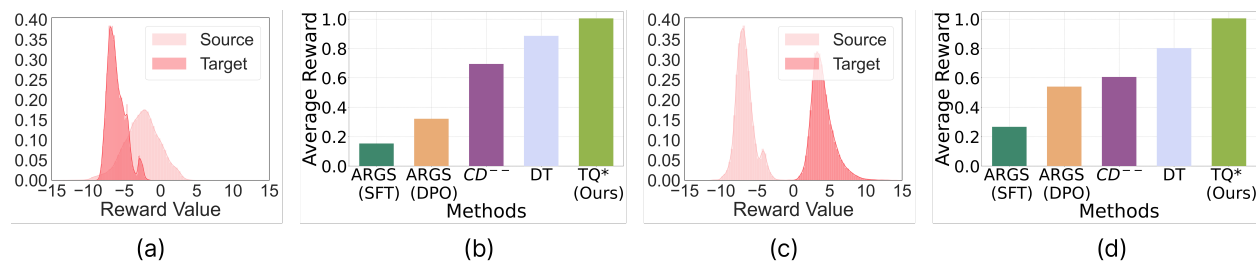


Figure 5: **Evaluation for Real Indirect Transfer Tasks.** In (a) and (c), we visualize the distribution shift in reward values between the source and target for Setup-1 and Setup-2, respectively, as outlined in Table 5. In (b) and (d), we report the normalized average reward scores of different decoding strategies corresponding to Setup-1 and Setup-2, respectively.

## 5 Conclusions

In this paper, we introduce Transfer  $Q^*$ , a novel decoding strategy for AI alignment. Our method effectively addresses the prior gaps in alignment via decoding by leveraging an estimate of optimal  $Q^*$  for a target reward through an existing aligned policy  $\rho_{BL}$ . Our theoretical analysis provides a rigorous characterization of the sub-optimality gap with respect to the token-level value function and the KL divergence to the reference policy. Experimentally, we demonstrate the consistent and significant superiority of the proposed approach. Hence, this work provides a principled solution to efficient decoding for AI alignment.

## 6 Acknowledgments

Chakraborty and Huang are supported by DARPA Transfer from Imprecise and Abstract Models to Autonomous Technologies (TIAMAT) 80321, National Science Foundation NSF-IIS-2147276 FAI, DOD-ONR-Office of Naval Research under award number N00014-22-1-2335, DOD-AFOSR-Air Force Office of Scientific Research under award number FA9550-23-1-0048, DOD-DARPA-Defense Advanced Research Projects Agency Guaranteeing AI Robustness against Deception (GARD) HR00112020007, Adobe, Capital One and JP Morgan faculty fellowships. Manocha and Bedi are supported by Army Cooperative Agreement W911NF2120076.

## References

- [1] Alekh Agarwal, Nan Jiang, Sham M Kakade, and Wen Sun. Reinforcement learning: Theory and algorithms. *CS Dept., UW Seattle, Seattle, WA, USA, Tech. Rep*, 32:96, 2019.
- [2] Amanda Askell, Yuntao Bai, Anna Chen, Dawn Drain, Deep Ganguli, Tom Henighan, Andy Jones, Nicholas Joseph, Ben Mann, Nova DasSarma, et al. A general language assistant as a laboratory for alignment. *arXiv preprint arXiv:2112.00861*, 2021.
- [3] Mohammad Gheshlaghi Azar, Mark Rowland, Bilal Piot, Daniel Guo, Daniele Calandriello, Michal Valko, and Rémi Munos. A general theoretical paradigm to understand learning from human preferences, 2023.
- [4] Dzmitry Bahdanau, Felix Hill, Jan Leike, Edward Hughes, Arian Hosseini, Pushmeet Kohli, and Edward Grefenstette. Learning to understand goal specifications by modelling reward. *arXiv preprint arXiv:1806.01946*, 2018.
- [5] Yuntao Bai, Andy Jones, Kamal Ndousse, Amanda Askell, Anna Chen, Nova DasSarma, Dawn Drain, Stanislav Fort, Deep Ganguli, Tom Henighan, et al. Training a helpful and harmless assistant with reinforcement learning from human feedback. *arXiv preprint arXiv:2204.05862*, 2022.
- [6] Tris Warkentin Jeanine Banks and Tris Warkentin. Gemma: Introducing new state-of-the-art open models, 2024.

- [7] Stella Biderman, Hailey Schoelkopf, Quentin Gregory Anthony, Herbie Bradley, Kyle O’Brien, Eric Hallahan, Mohammad Aflah Khan, Shivanshu Purohit, USVSN Sai Prashanth, Edward Raff, et al. Pythia: A suite for analyzing large language models across training and scaling. In *International Conference on Machine Learning*, pp. 2397–2430. PMLR, 2023.
- [8] Ralph Allan Bradley and Milton E Terry. Rank analysis of incomplete block designs: I. the method of paired comparisons. *Biometrika*, 39(3/4):324–345, 1952.
- [9] Souradip Chakraborty, Amrit Bedi, Alec Koppel, Huazheng Wang, Dinesh Manocha, Mengdi Wang, and Furong Huang. Parl: A unified framework for policy alignment in reinforcement learning. In *The Twelfth International Conference on Learning Representations (ICLR)*, 2024.
- [10] Zixiang Chen, Yihe Deng, Huizhuo Yuan, Kaixuan Ji, and Quanquan Gu. Self-play fine-tuning converts weak language models to strong language models. *arXiv preprint arXiv:2401.01335*, 2024.
- [11] Paul F Christiano, Jan Leike, Tom Brown, Miljan Martic, Shane Legg, and Dario Amodei. Deep reinforcement learning from human preferences. *Advances in neural information processing systems*, 30, 2017.
- [12] Ganqu Cui, Lifan Yuan, Ning Ding, Guanming Yao, Wei Zhu, Yuan Ni, Guotong Xie, Zhiyuan Liu, and Maosong Sun. Ultrafeedback: Boosting language models with high-quality feedback. *arXiv preprint arXiv:2310.01377*, 2023.
- [13] Josef Dai, Xuehai Pan, Ruiyang Sun, Jiaming Ji, Xinbo Xu, Mickel Liu, Yizhou Wang, and Yaodong Yang. Safe rlhf: Safe reinforcement learning from human feedback, 2023.
- [14] Hanze Dong, Wei Xiong, Deepanshu Goyal, Yihan Zhang, Winnie Chow, Rui Pan, Shizhe Diao, Jipeng Zhang, Kashun Shum, and Tong Zhang. Raft: Reward ranked finetuning for generative foundation model alignment. *arXiv preprint arXiv:2304.06767*, 2023.
- [15] Ahmad Faiz, Sotaro Kaneda, Ruhan Wang, Rita Osi, Prateek Sharma, Fan Chen, and Lei Jiang. Llmcarbon: Modeling the end-to-end carbon footprint of large language models, 2024.
- [16] Angela Fan, Mike Lewis, and Yann Dauphin. Hierarchical neural story generation, 2018.
- [17] Markus Freitag and Yaser Al-Onaizan. Beam search strategies for neural machine translation. *arXiv preprint arXiv:1702.01806*, 2017.
- [18] Leo Gao, John Schulman, and Jacob Hilton. Scaling laws for reward model overoptimization. In *International Conference on Machine Learning*, pp. 10835–10866. PMLR, 2023.
- [19] Amelia Glaese, Nat McAleese, Maja Trębacz, John Aslanides, Vlad Firoiu, Timo Ewalds, Maribeth Rauh, Laura Weidinger, Martin Chadwick, Phoebe Thacker, et al. Improving alignment of dialogue agents via targeted human judgements. *arXiv preprint arXiv:2209.14375*, 2022.
- [20] Ari Holtzman, Jan Buys, Li Du, Maxwell Forbes, and Yejin Choi. The curious case of neural text degeneration. *arXiv preprint arXiv:1904.09751*, 2019.

- [21] James Y Huang, Sailik Sengupta, Daniele Bonadiman, Yi-an Lai, Arshit Gupta, Nikolaos Pappas, Saab Mansour, Katrin Kirchoff, and Dan Roth. Deal: Decoding-time alignment for large language models. *arXiv preprint arXiv:2402.06147*, 2024.
- [22] Borja Ibarz, Jan Leike, Tobias Pohlen, Geoffrey Irving, Shane Legg, and Dario Amodei. Reward learning from human preferences and demonstrations in atari. *Advances in neural information processing systems*, 31, 2018.
- [23] Hamish Ivison, Yizhong Wang, Valentina Pyatkin, Nathan Lambert, Matthew Peters, Pradeep Dasigi, Joel Jang, David Wadden, Noah A Smith, Iz Beltagy, et al. Camels in a changing climate: Enhancing lm adaptation with tulu 2. *arXiv preprint arXiv:2311.10702*, 2023.
- [24] Albert Q Jiang, Alexandre Sablayrolles, Arthur Mensch, Chris Bamford, Devendra Singh Chaplot, Diego de las Casas, Florian Bressand, Gianna Lengyel, Guillaume Lample, Lucile Saulnier, et al. Mistral 7b. *arXiv preprint arXiv:2310.06825*, 2023.
- [25] Jared Kaplan, Sam McCandlish, Tom Henighan, Tom B. Brown, Benjamin Chess, Rewon Child, Scott Gray, Alec Radford, Jeffrey Wu, and Dario Amodei. Scaling laws for neural language models, 2020.
- [26] Maxim Khanov, Jirayu Burapachee, and Yixuan Li. Args: Alignment as reward-guided search, 2024.
- [27] Nathan Lambert, Valentina Pyatkin, Jacob Morrison, LJ Miranda, Bill Yuchen Lin, Khyathi Chandu, Nouha Dziri, Sachin Kumar, Tom Zick, Yejin Choi, Noah A. Smith, and Hannaneh Hajishirzi. Rewardbench: Evaluating reward models for language modeling, 2024.
- [28] Hao Liu, Carmelo Sferrazza, and Pieter Abbeel. Chain of hindsight aligns language models with feedback. *arXiv preprint arXiv:2302.02676*, 2023.
- [29] Tianlin Liu, Shangmin Guo, Leonardo Bianco, Daniele Calandriello, Quentin Berthet, Felipe Llinares, Jessica Hoffmann, Lucas Dixon, Michal Valko, and Mathieu Blondel. Decoding-time realignment of language models. *arXiv preprint arXiv:2402.02992*, 2024.
- [30] James MacGlashan, Mark K Ho, Robert Loftin, Bei Peng, Guan Wang, David L Roberts, Matthew E Taylor, and Michael L Littman. Interactive learning from policy-dependent human feedback. In *International conference on machine learning*, pp. 2285–2294. PMLR, 2017.
- [31] Shervin Minaee, Tomas Mikolov, Narjes Nikzad, Meysam Chenaghlu, Richard Socher, Xavier Amatriain, and Jianfeng Gao. Large language models: A survey, 2024.
- [32] Tetsuro Morimura, Mitsuki Sakamoto, Yuu Jinnai, Kenshi Abe, and Kaito Ariu. Filtered direct preference optimization, 2024.
- [33] Sidharth Mudgal, Jong Lee, Harish Ganapathy, YaGuang Li, Tao Wang, Yanping Huang, Zhifeng Chen, Heng-Tze Cheng, Michael Collins, Trevor Strohman, Jilin Chen, Alex Beutel, and Ahmad Beirami. Controlled decoding from language models, 2024.



- [34] Rémi Munos, Michal Valko, Daniele Calandriello, Mohammad Gheshlaghi Azar, Mark Rowland, Zhaohan Daniel Guo, Yunhao Tang, Matthieu Geist, Thomas Mesnard, Andrea Michi, Marco Selvi, Sertan Girgin, Nikola Momchev, Olivier Bachem, Daniel J. Mankowitz, Doina Precup, and Bilal Piot. Nash learning from human feedback, 2023.
- [35] Reiichiro Nakano, Jacob Hilton, Suchir Balaji, Jeff Wu, Long Ouyang, Christina Kim, Christopher Hesse, Shantanu Jain, Vineet Kosaraju, William Saunders, et al. Webgpt: Browser-assisted question-answering with human feedback. *arXiv preprint arXiv:2112.09332*, 2021.
- [36] OpenAI, Josh Achiam, Steven Adler, Sandhini Agarwal, Lama Ahmad, Ilge Akkaya, Florencia Leoni Aleman, Diogo Almeida, Janko Altenschmidt, Sam Altman, Shyamal Anadkat, Red Avila, Igor Babuschkin, Suchir Balaji, Valerie Balcom, Paul Baltescu, Haiming Bao, Mohammad Bavarian, Jeff Belgum, Irwan Bello, Jake Berdine, Gabriel Bernadett-Shapiro, Christopher Berner, Lenny Bogdonoff, Oleg Boiko, Madelaine Boyd, Anna-Luisa Brakman, Greg Brockman, Tim Brooks, Miles Brundage, Kevin Button, Trevor Cai, Rosie Campbell, Andrew Cann, Brittany Carey, Chelsea Carlson, Rory Carmichael, Brooke Chan, Che Chang, Fotis Chantzis, Derek Chen, Sully Chen, Ruby Chen, Jason Chen, Mark Chen, Ben Chess, Chester Cho, Casey Chu, Hyung Won Chung, Dave Cummings, Jeremiah Currier, Yunxing Dai, Cory Decareaux, Thomas Degry, Noah Deutsch, Damien Deville, Arka Dhar, David Dohan, Steve Dowling, Sheila Dunning, Adrien Ecoffet, Atty Eleti, Tyna Eloundou, David Farhi, Liam Fedus, Niko Felix, Simón Posada Fishman, Juston Forte, Isabella Fulford, Leo Gao, Elie Georges, Christian Gibson, Vik Goel, Tarun Gogineni, Gabriel Goh, Rapha Gontijo-Lopes, Jonathan Gordon, Morgan Grafstein, Scott Gray, Ryan Greene, Joshua Gross, Shixiang Shane Gu, Yufei Guo, Chris Hallacy, Jesse Han, Jeff Harris, Yuchen He, Mike Heaton, Johannes Heidecke, Chris Hesse, Alan Hickey, Wade Hickey, Peter Hoeschele, Brandon Houghton, Kenny Hsu, Shengli Hu, Xin Hu, Joost Huizinga, Shantanu Jain, Shawn Jain, Joanne Jang, Angela Jiang, Roger Jiang, Haozhun Jin, Denny Jin, Shino Jomoto, Billie Jonn, Heewoo Jun, Tomer Kaftan, Łukasz Kaiser, Ali Kamali, Ingmar Kanitscheider, Nitish Shirish Keskar, Tabarak Khan, Logan Kilpatrick, Jong Wook Kim, Christina Kim, Yongjik Kim, Jan Hendrik Kirchner, Jamie Kiros, Matt Knight, Daniel Kokotajlo, Łukasz Kondraciuk, Andrew Kondrich, Aris Konstantinidis, Kyle Kosic, Gretchen Krueger, Vishal Kuo, Michael Lampe, Ikai Lan, Teddy Lee, Jan Leike, Jade Leung, Daniel Levy, Chak Ming Li, Rachel Lim, Molly Lin, Stephanie Lin, Mateusz Litwin, Theresa Lopez, Ryan Lowe, Patricia Lue, Anna Makanju, Kim Malfacini, Sam Manning, Todor Markov, Yaniv Markovski, Bianca Martin, Katie Mayer, Andrew Mayne, Bob McGrew, Scott Mayer McKinney, Christine McLeavey, Paul McMillan, Jake McNeil, David Medina, Aalok Mehta, Jacob Menick, Luke Metz, Andrey Mishchenko, Pamela Mishkin, Vinnie Monaco, Evan Morikawa, Daniel Mossing, Tong Mu, Mira Murati, Oleg Murk, David Mély, Ashvin Nair, Reiichiro Nakano, Rajeev Nayak, Arvind Neelakantan, Richard Ngo, Hyeonwoo Noh, Long Ouyang, Cullen O’Keefe, Jakub Pachocki, Alex Paino, Joe Palermo, Ashley Pantuliano, Giambattista Parascandolo, Joel Parish, Emy Parparita, Alex Passos, Mikhail Pavlov, Andrew Peng, Adam Perelman, Filipe de Avila Belbute Peres, Michael Petrov, Henrique Ponde de Oliveira Pinto, Michael, Pokorny, Michelle Pokrass, Vitchyr H. Pong, Tolly Powell, Alethea Power, Boris Power, Elizabeth Proehl, Raul Puri, Alec Radford, Jack Rae, Aditya Ramesh, Cameron Raymond, Francis Real, Kendra Rimbach, Carl Ross, Bob Rotsted, Henri Roussez, Nick Ryder, Mario Saltarelli, Ted Sanders, Shibani Santurkar, Girish

- Sastry, Heather Schmidt, David Schnurr, John Schulman, Daniel Selsam, Kyla Sheppard, Toki Sherbakov, Jessica Shieh, Sarah Shoker, Pranav Shyam, Szymon Sidor, Eric Sigler, Maddie Simens, Jordan Sitkin, Katarina Slama, Ian Sohl, Benjamin Sokolowsky, Yang Song, Natalie Staudacher, Felipe Petroski Such, Natalie Summers, Ilya Sutskever, Jie Tang, Nikolas Tezak, Madeleine B. Thompson, Phil Tillet, Amin Tootoonchian, Elizabeth Tseng, Preston Tuggle, Nick Turley, Jerry Tworek, Juan Felipe Cerón Uribe, Andrea Vallone, Arun Vijayvergiya, Chelsea Voss, Carroll Wainwright, Justin Jay Wang, Alvin Wang, Ben Wang, Jonathan Ward, Jason Wei, CJ Weinmann, Akila Welihinda, Peter Welinder, Jiayi Weng, Lilian Weng, Matt Wiethoff, Dave Willner, Clemens Winter, Samuel Wolrich, Hannah Wong, Lauren Workman, Sherwin Wu, Jeff Wu, Michael Wu, Kai Xiao, Tao Xu, Sarah Yoo, Kevin Yu, Qiming Yuan, Wojciech Zaremba, Rowan Zellers, Chong Zhang, Marvin Zhang, Shengjia Zhao, Tianhao Zheng, Juntang Zhuang, William Zhuk, and Barret Zoph. Gpt-4 technical report, 2024.
- [37] Long Ouyang, Jeff Wu, Xu Jiang, Diogo Almeida, Carroll L. Wainwright, Pamela Mishkin, Chong Zhang, Sandhini Agarwal, Katarina Slama, Alex Ray, John Schulman, Jacob Hilton, Fraser Kelton, Luke Miller, Maddie Simens, Amanda Askell, Peter Welinder, Paul Christiano, Jan Leike, and Ryan Lowe. Training language models to follow instructions with human feedback, 2022.
- [38] Rafael Rafailov, Archit Sharma, Eric Mitchell, Stefano Ermon, Christopher D. Manning, and Chelsea Finn. Direct preference optimization: Your language model is secretly a reward model, 2023.
- [39] Charlie Snell, Ilya Kostrikov, Yi Su, Mengjiao Yang, and Sergey Levine. Offline rl for natural language generation with implicit language q learning. *arXiv preprint arXiv:2206.11871*, 2022.
- [40] Nisan Stiennon, Long Ouyang, Jeffrey Wu, Daniel Ziegler, Ryan Lowe, Chelsea Voss, Alec Radford, Dario Amodei, and Paul F Christiano. Learning to summarize with human feedback. *Advances in Neural Information Processing Systems*, 33:3008–3021, 2020.
- [41] Nisan Stiennon, Long Ouyang, Jeff Wu, Daniel M. Ziegler, Ryan Lowe, Chelsea Voss, Alec Radford, Dario Amodei, and Paul Christiano. Learning to summarize from human feedback, 2022.
- [42] Nisan Stiennon, Long Ouyang, Jeff Wu, Daniel M. Ziegler, Ryan Lowe, Chelsea Voss, Alec Radford, Dario Amodei, and Paul Christiano. Learning to summarize from human feedback, 2022.
- [43] Yixuan Su, Tian Lan, Yan Wang, Dani Yogatama, Lingpeng Kong, and Nigel Collier. A contrastive framework for neural text generation. In Alice H. Oh, Alekh Agarwal, Danielle Belgrave, and Kyunghyun Cho (eds.), *Advances in Neural Information Processing Systems*, 2022.
- [44] Gemini Team, Rohan Anil, Sebastian Borgeaud, Jean-Baptiste Alayrac, Jiahui Yu, Radu Soricut, Johan Schalkwyk, Andrew M. Dai, Anja Hauth, Katie Millican, David Silver, Melvin Johnson, Ioannis Antonoglou, Julian Schrittwieser, Amelia Glaese, Jilin Chen, Emily Pitler, Timothy Lillicrap, Angeliki Lazaridou, Orhan Firat, James Molloy, Michael Isard, Paul R.

Barham, Tom Hennigan, Benjamin Lee, Fabio Viola, Malcolm Reynolds, Yuanzhong Xu, Ryan Doherty, Eli Collins, Clemens Meyer, Eliza Rutherford, Erica Moreira, Kareem Ayoub, Megha Goel, Jack Krawczyk, Cosmo Du, Ed Chi, Heng-Tze Cheng, Eric Ni, Purvi Shah, Patrick Kane, Betty Chan, Manaal Faruqui, Aliaksei Severyn, Hanzhao Lin, YaGuang Li, Yong Cheng, Abe Ittycheriah, Mahdis Mahdieh, Mia Chen, Pei Sun, Dustin Tran, Sumit Bagri, Balaji Lakshminarayanan, Jeremiah Liu, Andras Orban, Fabian Gra, Hao Zhou, Xinying Song, Aurelien Boffy, Harish Ganapathy, Steven Zheng, HyunJeong Choe, Ágoston Weisz, Tao Zhu, Yifeng Lu, Siddharth Gopal, Jarrod Kahn, Maciej Kula, Jeff Pitman, Rushin Shah, Emanuel Taropa, Majd Al Merey, Martin Baeuml, Zhifeng Chen, Laurent El Shafey, Yujing Zhang, Olcan Sercinoglu, George Tucker, Enrique Piqueras, Maxim Krikun, Iain Barr, Nikolay Savinov, Ivo Danihelka, Becca Roelofs, Anas White, Anders Andreassen, Tamara von Glehn, Lakshman Yagati, Mehran Kazemi, Lucas Gonzalez, Misha Khalman, Jakub Sygnowski, Alexandre Frechette, Charlotte Smith, Laura Culp, Lev Proleev, Yi Luan, Xi Chen, James Lottes, Nathan Schucher, Federico Lebron, Alban Rrustemi, Natalie Clay, Phil Crone, Tomas Kocisky, Jeffrey Zhao, Bartek Perz, Dian Yu, Heidi Howard, Adam Bloniarz, Jack W. Rae, Han Lu, Laurent Sifre, Marcello Maggioni, Fred Alcober, Dan Garrette, Megan Barnes, Shantanu Thakoor, Jacob Austin, Gabriel Barth-Maron, William Wong, Rishabh Joshi, Rahma Chaabouni, Deeni Fatiha, Arun Ahuja, Gaurav Singh Tomar, Evan Senter, Martin Chadwick, Ilya Kornakov, Nithya Attaluri, Iaki Iturrate, Ruibo Liu, Yunxuan Li, Sarah Cogan, Jeremy Chen, Chao Jia, Chenjie Gu, Qiao Zhang, Jordan Grimstad, Ale Jakse Hartman, Xavier Garcia, Thanumalayan Sankaranarayana Pillai, Jacob Devlin, Michael Laskin, Diego de Las Casas, Dasha Valter, Connie Tao, Lorenzo Blanco, Adri Puigdomnech Badia, David Reitter, Mianna Chen, Jenny Brennan, Clara Rivera, Sergey Brin, Shariq Iqbal, Gabriela Surita, Jane Labanowski, Abhi Rao, Stephanie Winkler, Emilio Parisotto, Yiming Gu, Kate Olszewska, Ravi Addanki, Antoine Miech, Annie Louis, Denis Teplyashin, Geoff Brown, Elliot Catt, Jan Balaguer, Jackie Xiang, Pidong Wang, Zoe Ashwood, Anton Briukhov, Albert Webson, Sanjay Ganapathy, Smit Sanghavi, Ajay Kannan, Ming-Wei Chang, Axel Stjerngren, Josip Djolonga, Yuting Sun, Ankur Bapna, Matthew Aitchison, Pedram Pejman, Henryk Michalewski, Tianhe Yu, Cindy Wang, Juliette Love, Junwhan Ahn, Dawn Bloxwich, Kehang Han, Peter Humphreys, Thibault Sellam, James Bradbury, Varun Godbole, Sina Samangooei, Bogdan Damoc, Alex Kaskasoli, Sbastien M. R. Arnold, Vijay Vasudevan, Shubham Agrawal, Jason Riesa, Dmitry Lepikhin, Richard Tanburn, Srivatsan Srinivasan, Hyeontaek Lim, Sarah Hodkinson, Pranav Shyam, Johan Ferret, Steven Hand, Ankush Garg, Tom Le Paine, Jian Li, Yujia Li, Minh Giang, Alexander Neitz, Zaheer Abbas, Sarah York, Machel Reid, Elizabeth Cole, Aakanksha Chowdhery, Dipanjan Das, Dominika Rogoziska, Vitaliy Nikolaev, Pablo Sprechmann, Zachary Nado, Lukas Zilka, Flavien Prost, Luheng He, Marianne Monteiro, Gaurav Mishra, Chris Welty, Josh Newlan, Dawei Jia, Miltiadis Allamanis, Clara Huiyi Hu, Raoul de Liedekerke, Justin Gilmer, Carl Saroufim, Shruti Rijhwani, Shaobo Hou, Disha Shrivastava, Anirudh Baddepudi, Alex Goldin, Adnan Ozturel, Albin Cassirer, Yunhan Xu, Daniel Sohn, Devendra Sachan, Reinald Kim Amplayo, Craig Swanson, Dessie Petrova, Shashi Narayan, Arthur Guez, Siddhartha Brahma, Jessica Landon, Miteyan Patel, Ruizhe Zhao, Kevin Vilella, Luyu Wang, Wenhao Jia, Matthew Rahtz, Mai Gimnez, Legg Yeung, James Keeling, Petko Georgiev, Diana Mincu, Boxi Wu, Salem Haykal, Rachel Saputro, Kiran Vodrahalli, James Qin, Zeynep Cankara, Abhanshu Sharma, Nick Fernando, Will Hawkins, Behnam Neyshabur, Solomon Kim, Adrian Hutter, Priyanka Agrawal, Alex Castro-Ros, George van den Driessche, Tao Wang, Fan Yang, Shuo

yiin Chang, Paul Komarek, Ross McIlroy, Mario Lučić, Guodong Zhang, Wael Farhan, Michael Sharman, Paul Natsev, Paul Michel, Yamini Bansal, Siyuan Qiao, Kris Cao, Siamak Shakeri, Christina Butterfield, Justin Chung, Paul Kishan Rubenstein, Shivani Agrawal, Arthur Mensch, Kedar Soparkar, Karel Lenc, Timothy Chung, Aedan Pope, Loren Maggiore, Jackie Kay, Priya Jhakra, Shibo Wang, Joshua Maynez, Mary Phuong, Taylor Tobin, Andrea Tacchetti, Maja Trebacz, Kevin Robinson, Yash Katariya, Sebastian Riedel, Paige Bailey, Kefan Xiao, Nimesh Ghelani, Lora Aroyo, Ambrose Slone, Neil Houlsby, Xuehan Xiong, Zhen Yang, Elena Gribovskaya, Jonas Adler, Mateo Wirth, Lisa Lee, Music Li, Thais Kagohara, Jay Pavagadhi, Sophie Bridgers, Anna Bortsova, Sanjay Ghemawat, Zafarali Ahmed, Tianqi Liu, Richard Powell, Vijay Bolina, Mariko Iinuma, Polina Zablotskaia, James Besley, Da-Woon Chung, Timothy Dozat, Ramona Comanescu, Xiance Si, Jeremy Greer, Guolong Su, Martin Polacek, Raphaël Lopez Kaufman, Simon Tokumine, Hexiang Hu, Elena Buchatskaya, Yingjie Miao, Mohamed Elhawaty, Aditya Siddhant, Nenad Tomasev, Jinwei Xing, Christina Greer, Helen Miller, Shereen Ashraf, Aurko Roy, Zizhao Zhang, Ada Ma, Angelos Filos, Milos Besta, Rory Blevins, Ted Klimenko, Chih-Kuan Yeh, Soravit Changpinyo, Jiaqi Mu, Oscar Chang, Mantas Pajarskas, Carrie Muir, Vered Cohen, Charline Le Lan, Krishna Haridasan, Amit Marathe, Steven Hansen, Sholto Douglas, Rajkumar Samuel, Mingqiu Wang, Sophia Austin, Chang Lan, Jiepu Jiang, Justin Chiu, Jaime Alonso Lorenzo, Lars Lowe Sjöstrand, Sébastien Cevey, Zach Gleicher, Thi Avrahami, Anudhyan Boral, Hansa Srinivasan, Vittorio Selo, Rhys May, Konstantinos Aisopos, Léonard Hussenot, Livio Baldini Soares, Kate Baumli, Michael B. Chang, Adrià Recasens, Ben Caine, Alexander Pritzel, Filip Pavetic, Fabio Pardo, Anita Gergely, Justin Frye, Vinay Ramasesh, Dan Horgan, Kartikeya Badola, Nora Kassner, Subhrajit Roy, Ethan Dyer, Víctor Campos Campos, Alex Tomala, Yunhao Tang, Dalia El Badawy, Elspeth White, Basil Mustafa, Oran Lang, Abhishek Jindal, Sharad Vikram, Zhitao Gong, Sergi Caelles, Ross Hemsley, Gregory Thornton, Fangxiaoyu Feng, Wojciech Stokowiec, Ce Zheng, Phoebe Thacker, Çağlar Ünlü, Zhishuai Zhang, Mohammad Saleh, James Svensson, Max Bileschi, Piyush Patil, Ankesh Anand, Roman Ring, Katerina Tsihlias, Arpi Vezer, Marco Selvi, Toby Shevlane, Mikel Rodriguez, Tom Kwiatkowski, Samira Daruki, Keran Rong, Allan Dafoe, Nicholas FitzGerald, Keren Gu-Lemberg, Mina Khan, Lisa Anne Hendricks, Marie Pellat, Vladimir Feinberg, James Cobon-Kerr, Tara Sainath, Maribeth Rauh, Sayed Hadi Hashemi, Richard Ives, Yana Hasson, Eric Noland, Yuan Cao, Nathan Byrd, Le Hou, Qingze Wang, Thibault Sottiaux, Michela Paganini, Jean-Baptiste Lespiau, Alexandre Moufarek, Samer Hassan, Kaushik Shivakumar, Joost van Amersfoort, Amol Mandhane, Pratik Joshi, Anirudh Goyal, Matthew Tung, Andrew Brock, Hannah Sheahan, Vedant Misra, Cheng Li, Nemanja Rakićević, Mostafa Dehghani, Fangyu Liu, Sid Mittal, Junhyuk Oh, Seb Noury, Eren Sezener, Fantine Huot, Matthew Lamm, Nicola De Cao, Charlie Chen, Sidharth Mudgal, Romina Stella, Kevin Brooks, Gautam Vasudevan, Chenxi Liu, Mainak Chain, Nivedita Melinkeri, Aaron Cohen, Venus Wang, Kristie Seymore, Sergey Zubkov, Rahul Goel, Summer Yue, Sai Krishnakumaran, Brian Albert, Nate Hurley, Motoki Sano, Anhad Mohananey, Jonah Joughin, Egor Filonov, Tomasz Kępa, Yomna Eldawy, Jiawern Lim, Rahul Rishi, Shirin Badiezhadegan, Taylor Bos, Jerry Chang, Sanil Jain, Sri Gayatri Sundara Padmanabhan, Subha Puttagunta, Kalpesh Krishna, Leslie Baker, Norbert Kalb, Vamsi Bedapudi, Adam Kurzrok, Shuntong Lei, Anthony Yu, Oren Litvin, Xiang Zhou, Zhichun Wu, Sam Sobell, Andrea Siciliano, Alan Papir, Robby Neale, Jonas Bragagnolo, Tej Toor, Tina Chen, Valentin Anklin, Feiran Wang, Richie Feng, Milad Gholami, Kevin Ling, Lijuan Liu, Jules Walter, Hamid Moghaddam, Arun Kishore,

Jakub Adamek, Tyler Mercado, Jonathan Mallinson, Siddhinita Wandekar, Stephen Cagle, Eran Ofek, Guillermo Garrido, Clemens Lombriser, Maksim Mukha, Botu Sun, Hafeezul Rahman Mohammad, Josip Matak, Yadi Qian, Vikas Peswani, Pawel Janus, Quan Yuan, Leif Schelin, Oana David, Ankur Garg, Yifan He, Oleksii Duzhyi, Anton Älgmyr, Timothée Lottaz, Qi Li, Vikas Yadav, Luyao Xu, Alex Chinien, Rakesh Shivanna, Aleksandr Chuklin, Josie Li, Carrie Spadine, Travis Wolfe, Kareem Mohamed, Subhabrata Das, Zihang Dai, Kyle He, Daniel von Dincklage, Shyam Upadhyay, Akanksha Maurya, Luyan Chi, Sebastian Krause, Khalid Salama, Pam G Rabinovitch, Pavan Kumar Reddy M, Aarush Selvan, Mikhail Dektiarev, Golnaz Ghiasi, Erdem Guven, Himanshu Gupta, Boyi Liu, Deepak Sharma, Idan Heimlich Shtacher, Shachi Paul, Oscar Akerlund, François-Xavier Aubet, Terry Huang, Chen Zhu, Eric Zhu, Elico Teixeira, Matthew Fritze, Francesco Bertolini, Liana-Eleonora Marinescu, Martin Bölle, Dominik Paulus, Khyatti Gupta, Tejasi Latkar, Max Chang, Jason Sanders, Roopa Wilson, Xuewei Wu, Yi-Xuan Tan, Lam Nguyen Thiet, Tulsee Doshi, Sid Lall, Swaroop Mishra, Wanming Chen, Thang Luong, Seth Benjamin, Jasmine Lee, Ewa Andrejczuk, Dominik Rabiej, Vipul Ranjan, Krzysztof Styrz, Pengcheng Yin, Jon Simon, Malcolm Rose Harriott, Mudit Bansal, Alexei Robsky, Geoff Bacon, David Greene, Daniil Mirylenka, Chen Zhou, Obaid Sarvana, Abhimanyu Goyal, Samuel Andermatt, Patrick Siegler, Ben Horn, Assaf Israel, Francesco Pongetti, Chih-Wei "Louis" Chen, Marco Selvatici, Pedro Silva, Kathie Wang, Jackson Tolins, Kelvin Guu, Roey Yogev, Xiaochen Cai, Alessandro Agostini, Maulik Shah, Hung Nguyen, Noah Ó Donnaile, Sébastien Pereira, Linda Friso, Adam Stambler, Adam Kurzrok, Chenkai Kuang, Yan Romanikhin, Mark Geller, ZJ Yan, Kane Jang, Cheng-Chun Lee, Wojciech Fica, Eric Malmi, Qijun Tan, Dan Banica, Daniel Balle, Ryan Pham, Yanping Huang, Diana Avram, Hongzhi Shi, Jasjot Singh, Chris Hidey, Niharika Ahuja, Pranab Saxena, Dan Dooley, Srividya Pranavi Potharaju, Eileen O'Neill, Anand Gokulchandran, Ryan Foley, Kai Zhao, Mike Dusenberry, Yuan Liu, Pulkit Mehta, Ragha Kotikalapudi, Chalence Safranek-Shrader, Andrew Goodman, Joshua Kessinger, Eran Globen, Prateek Kolhar, Chris Gorgolewski, Ali Ibrahim, Yang Song, Ali Eichenbaum, Thomas Brovelli, Sahitya Potluri, Preethi Lahoti, Cip Baetu, Ali Ghorbani, Charles Chen, Andy Crawford, Shalini Pal, Mukund Sridhar, Petru Gurita, Asier Mujika, Igor Petrovski, Pierre-Louis Cedoz, Chenmei Li, Shiyuan Chen, Niccolò Dal Santo, Siddharth Goyal, Jitesh Punjabi, Karthik Kappaganthu, Chester Kwak, Pallavi LV, Sarmishta Velury, Himadri Choudhury, Jamie Hall, Premal Shah, Ricardo Figueira, Matt Thomas, Minjie Lu, Ting Zhou, Chintu Kumar, Thomas Jurdi, Sharat Chikkerur, Yenai Ma, Adams Yu, Soo Kwak, Victor Ähdel, Sujevan Rajayogam, Travis Choma, Fei Liu, Aditya Barua, Colin Ji, Ji Ho Park, Vincent Hellendoorn, Alex Bailey, Taylan Bilal, Huanjie Zhou, Mehrdad Khatir, Charles Sutton, Wojciech Rzadkowski, Fiona Macintosh, Konstantin Shagin, Paul Medina, Chen Liang, Jinjing Zhou, Pararth Shah, Yingying Bi, Attila Dankovics, Shipra Banga, Sabine Lehmann, Marissa Bredesen, Zifan Lin, John Eric Hoffmann, Jonathan Lai, Raynald Chung, Kai Yang, Nihal Balani, Arthur Bražinskas, Andrei Sozanschi, Matthew Hayes, Héctor Fernández Alcalde, Peter Makarov, Will Chen, Antonio Stella, Liselotte Snijders, Michael Mandl, Ante Kärrman, Paweł Nowak, Xinyi Wu, Alex Dyck, Krishnan Vaidyanathan, Raghavender R, Jessica Mallet, Mitch Rudominer, Eric Johnston, Sushil Mittal, Akhil Udathu, Janara Christensen, Vishal Verma, Zach Irving, Andreas Santucci, Gamaleldin Elsayed, Elnaz Davoodi, Marin Georgiev, Ian Tenney, Nan Hua, Geoffrey Cideron, Edouard Leurent, Mahmoud Alnahlawi, Ionut Georgescu, Nan Wei, Ivy Zheng, Dylan Scandinaro, Heinrich Jiang, Jasper Snoek, Mukund Sundararajan, Xuezhi Wang, Zack Ontiveros, Itay Karo, Jeremy Cole, Vinu

Rajashekhar, Lara Tumeah, Eyal Ben-David, Rishub Jain, Jonathan Uesato, Romina Datta, Oskar Bunyan, Shimu Wu, John Zhang, Piotr Stanczyk, Ye Zhang, David Steiner, Subhajit Naskar, Michael Azzam, Matthew Johnson, Adam Paszke, Chung-Cheng Chiu, Jaume Sanchez Elias, Afroz Mohiuddin, Faizan Muhammad, Jin Miao, Andrew Lee, Nino Vieillard, Jane Park, Jiageng Zhang, Jeff Stanway, Drew Garmon, Abhijit Karmarkar, Zhe Dong, Jong Lee, Aviral Kumar, Luowei Zhou, Jonathan Evens, William Isaac, Geoffrey Irving, Edward Loper, Michael Fink, Isha Arkatkar, Nanxin Chen, Izhak Shafran, Ivan Petychenko, Zhe Chen, Johnson Jia, Anselm Levskaya, Zhenkai Zhu, Peter Grabowski, Yu Mao, Alberto Magni, Kaisheng Yao, Javier Snaider, Norman Casagrande, Evan Palmer, Paul Suganthan, Alfonso Castaño, Irene Giannoumis, Wooyeol Kim, Mikołaj Rybiński, Ashwin Sreevatsa, Jennifer Prendki, David Soergel, Adrian Goedeckemeyer, Willi Gierke, Mohsen Jafari, Meenu Gaba, Jeremy Wiesner, Diana Gage Wright, Yawen Wei, Harsha Vashisht, Yana Kulizhskaya, Jay Hoover, Maigo Le, Lu Li, Chimezie Iwuanyanwu, Lu Liu, Kevin Ramirez, Andrey Khorlin, Albert Cui, Tian LIN, Marcus Wu, Ricardo Aguilar, Keith Pallo, Abhishek Chakladar, Ginger Perng, Elena Allica Abellan, Mingyang Zhang, Ishita Dasgupta, Nate Kushman, Ivo Penchev, Alena Repina, Xihui Wu, Tom van der Weide, Priya Ponnappalli, Caroline Kaplan, Jiri Simsa, Shuangfeng Li, Olivier Dousse, Fan Yang, Jeff Piper, Nathan Ie, Rama Pasumarthi, Nathan Lintz, Anitha Vijayakumar, Daniel Andor, Pedro Valenzuela, Minnie Lui, Cosmin Paduraru, Daiyi Peng, Katherine Lee, Shuyuan Zhang, Somer Greene, Duc Dung Nguyen, Paula Kurylowicz, Cassidy Hardin, Lucas Dixon, Lili Janzer, Kiam Choo, Ziqiang Feng, Biao Zhang, Achintya Singhal, Dayou Du, Dan McKinnon, Natasha Antropova, Tolga Bolukbasi, Orgad Keller, David Reid, Daniel Finchelstein, Maria Abi Raad, Remi Crocker, Peter Hawkins, Robert Dadashi, Colin Gaffney, Ken Franko, Anna Bulanova, Rémi Leblond, Shirley Chung, Harry Askham, Luis C. Cobo, Kelvin Xu, Felix Fischer, Jun Xu, Christina Sorokin, Chris Alberti, Chu-Cheng Lin, Colin Evans, Alek Dimitriev, Hannah Forbes, Dylan Banarse, Zora Tung, Mark Omernick, Colton Bishop, Rachel Sterneck, Rohan Jain, Jiawei Xia, Ehsan Amid, Francesco Piccinno, Xingyu Wang, Praseem Banzal, Daniel J. Mankowitz, Alex Polozov, Victoria Krakovna, Sasha Brown, MohammadHossein Bateni, Dennis Duan, Vlad Firoiu, Meghana Thotakuri, Tom Natan, Matthieu Geist, Ser tan Girgin, Hui Li, Jiayu Ye, Ofir Roval, Reiko Tojo, Michael Kwong, James Lee-Thorp, Christopher Yew, Danila Sinopalnikov, Sabela Ramos, John Mellor, Abhishek Sharma, Kathy Wu, David Miller, Nicolas Sonnerat, Denis Vnukov, Rory Greig, Jennifer Beattie, Emily Caveness, Libin Bai, Julian Eisenschlos, Alex Korchemniy, Tomy Tsai, Mimi Jasarevic, Weize Kong, Phuong Dao, Zeyu Zheng, Frederick Liu, Fan Yang, Rui Zhu, Tian Huey Teh, Jason Sanmiya, Evgeny Gladchenko, Nejc Trdin, Daniel Toyama, Evan Rosen, Sasan Tavakkol, Linting Xue, Chen Elkind, Oliver Woodman, John Carpenter, George Papamakarios, Rupert Kemp, Sushant Kafle, Tanya Grunina, Rishika Sinha, Alice Talbert, Diane Wu, Denese Owusu-Afriyie, Cosmo Du, Chloe Thornton, Jordi Pont-Tuset, Pradyumna Narayana, Jing Li, Saaber Fatehi, John Wieting, Omar Ajmeri, Benigno Uria, Yeongil Ko, Laura Knight, Amélie Héliou, Ning Niu, Shane Gu, Chenxi Pang, Yeqing Li, Nir Levine, Ariel Stolovich, Rebeca Santamaria-Fernandez, Sonam Goenka, Wenny Yustalim, Robin Strudel, Ali Elqursh, Charlie Deck, Hyo Lee, Zonglin Li, Kyle Levin, Raphael Hoffmann, Dan Holtmann-Rice, Olivier Bachem, Sho Arora, Christy Koh, Soheil Hassas Yeganeh, Siim Pöder, Mukarram Tariq, Yanhua Sun, Lucian Ionita, Mojtaba Seyedhosseini, Pouya Tafti, Zhiyu Liu, Anmol Gulati, Jasmine Liu, Xinyu Ye, Bart Chrzaszcz, Lily Wang, Nikhil Sethi, Tianrun Li, Ben Brown, Shreya Singh, Wei Fan, Aaron Parisi, Joe Stanton, Vinod Koverkathu, Christopher A.



Choquette-Choo, Yunjie Li, TJ Lu, Abe Ittycheriah, Prakash Shroff, Mani Varadarajan, Sanaz Bahargam, Rob Willoughby, David Gaddy, Guillaume Desjardins, Marco Cornero, Brona Robenek, Bhavishya Mittal, Ben Albrecht, Ashish Shenoy, Fedor Moiseev, Henrik Jacobsson, Alireza Ghaffarkhah, Morgane Rivièrè, Alanna Walton, Clément Crepy, Alicia Parrish, Zongwei Zhou, Clement Farabet, Carey Radebaugh, Praveen Srinivasan, Claudia van der Salm, Andreas Fidjeland, Salvatore Scellato, Eri Latorre-Chimoto, Hanna Klimczak-Plucińska, David Bridson, Dario de Cesare, Tom Hudson, Piermaria Mendolicchio, Lexi Walker, Alex Morris, Matthew Mauger, Alexey Guseynov, Alison Reid, Seth Odoo, Lucia Loher, Victor Cotruta, Madhavi Yenugula, Dominik Grewe, Anastasia Petrushkina, Tom Duerig, Antonio Sanchez, Steve Yadlowsky, Amy Shen, Amir Globerson, Lynette Webb, Sahil Dua, Dong Li, Surya Bhupatiraju, Dan Hurt, Haroon Qureshi, Ananth Agarwal, Tomer Shani, Matan Eyal, Anuj Khare, Shreyas Rammohan Belle, Lei Wang, Chetan Tekur, Mihir Sanjay Kale, Jinliang Wei, Ruoxin Sang, Brennan Saeta, Tyler Liechty, Yi Sun, Yao Zhao, Stephan Lee, Pandu Nayak, Doug Fritz, Manish Reddy Vuyyuru, John Aslanides, Nidhi Vyas, Martin Wicke, Xiao Ma, Evgenii Eltyshev, Nina Martin, Hardie Cate, James Manyika, Keyvan Amiri, Yelin Kim, Xi Xiong, Kai Kang, Florian Luisier, Nilesh Tripuraneni, David Madras, Mandy Guo, Austin Waters, Oliver Wang, Joshua Ainslie, Jason Baldridge, Han Zhang, Garima Pruthi, Jakob Bauer, Feng Yang, Riham Mansour, Jason Gelman, Yang Xu, George Polovets, Ji Liu, Honglong Cai, Warren Chen, XiangHai Sheng, Emily Xue, Sherjil Ozair, Christof Angermueller, Xiaowei Li, Anoop Sinha, Weiren Wang, Julia Wiesinger, Emmanouil Koukoumidis, Yuan Tian, Anand Iyer, Madhu Gurumurthy, Mark Goldenson, Parashar Shah, MK Blake, Hongkun Yu, Anthony Urbanowicz, Jennimaria Palomaki, Chrisantha Fernando, Ken Durden, Harsh Mehta, Nikola Momchev, Elahe Rahimtoroghi, Maria Georgaki, Amit Raul, Sebastian Ruder, Morgan Redshaw, Jinhyuk Lee, Denny Zhou, Komal Jalan, Dinghua Li, Blake Hechtman, Parker Schuh, Milad Nasr, Kieran Milan, Vladimir Mikulik, Juliana Franco, Tim Green, Nam Nguyen, Joe Kelley, Aroma Mahendru, Andrea Hu, Joshua Howland, Ben Vargas, Jeffrey Hui, Kshitij Bansal, Vikram Rao, Rakesh Ghiya, Emma Wang, Ke Ye, Jean Michel Sarr, Melanie Moranski Preston, Madeleine Elish, Steve Li, Aakash Kaku, Jigar Gupta, Ice Pasupat, Da-Cheng Juan, Milan Someswar, Tejvi M., Xinyun Chen, Aida Amini, Alex Fabrikant, Eric Chu, Xuanyi Dong, Amruta Muthal, Senaka Buthpitiya, Sarthak Jauhari, Nan Hua, Urvashi Khandelwal, Ayal Hitron, Jie Ren, Larissa Rinaldi, Shahar Drath, Avigail Dabush, Nan-Jiang Jiang, Harshal Godhia, Uli Sachs, Anthony Chen, Yicheng Fan, Hagai Taitelbaum, Hila Noga, Zhuyun Dai, James Wang, Chen Liang, Jenny Hamer, Chun-Sung Ferng, Chenel Elkind, Aviel Atias, Paulina Lee, Vít Listík, Mathias Carlen, Jan van de Kerkhof, Marcin Pikus, Krunoslav Zaher, Paul Müller, Sasha Zykova, Richard Stefanec, Vitaly Gatsko, Christoph Hirnschall, Ashwin Sethi, Xingyu Federico Xu, Chetan Ahuja, Beth Tsai, Anca Stefanoiu, Bo Feng, Keshav Dhandhania, Manish Katyal, Akshay Gupta, Atharva Parulekar, Divya Pitta, Jing Zhao, Vivaan Bhatia, Yashodha Bhavnani, Omar Alhadlaq, Xiaolin Li, Peter Danenberg, Dennis Tu, Alex Pine, Vera Filippova, Abhipso Ghosh, Ben Limonchik, Bhargava Urala, Chaitanya Krishna Lanka, Derik Clive, Yi Sun, Edward Li, Hao Wu, Kevin Hongtongsak, Ianna Li, Kalind Thakkar, Kuanysh Omarov, Kushal Majmundar, Michael Alverson, Michael Kucharski, Mohak Patel, Mudit Jain, Maksim Zabelin, Paolo Pelagatti, Rohan Kohli, Saurabh Kumar, Joseph Kim, Swetha Sankar, Vineet Shah, Lakshmi Ramachandrani, Xiangkai Zeng, Ben Bariach, Laura Weidinger, Amar Subramanya, Sissie Hsiao, Demis Hassabis, Koray Kavukcuoglu, Adam Sadovsky, Quoc Le, Trevor Strohman, Yonghui Wu, Slav Petrov, Jeffrey Dean, and Oriol Vinyals. Gemini: A family

of highly capable multimodal models, 2024.

- [45] Hugo Touvron, Thibaut Lavril, Gautier Izacard, Xavier Martinet, Marie-Anne Lachaux, Timothée Lacroix, Baptiste Rozière, Naman Goyal, Eric Hambro, Faisal Azhar, Aurelien Rodriguez, Armand Joulin, Edouard Grave, and Guillaume Lample. Llama: Open and efficient foundation language models, 2023.
- [46] Lewis Tunstall, Edward Beeching, Nathan Lambert, Nazneen Rajani, Kashif Rasul, Younes Belkada, Shengyi Huang, Leandro von Werra, Clémentine Fourrier, Nathan Habib, et al. Zephyr: Direct distillation of lm alignment. *arXiv preprint arXiv:2310.16944*, 2023.
- [47] Guan Wang, Sijie Cheng, Xianyuan Zhan, Xiangang Li, Sen Song, and Yang Liu. Openchat: Advancing open-source language models with mixed-quality data. *arXiv preprint arXiv:2309.11235*, 2023.
- [48] Tengyang Xie, Ching-An Cheng, Nan Jiang, Paul Mineiro, and Alekh Agarwal. Bellman-consistent pessimism for offline reinforcement learning. *Advances in neural information processing systems*, 34:6683–6694, 2021.
- [49] Ming Yin and Yu-Xiang Wang. Towards instance-optimal offline reinforcement learning with pessimism. *Advances in neural information processing systems*, 34:4065–4078, 2021.
- [50] Ming Yin, Yu Bai, and Yu-Xiang Wang. Near-optimal provable uniform convergence in offline policy evaluation for reinforcement learning. In *International Conference on Artificial Intelligence and Statistics*, pp. 1567–1575. PMLR, 2021.
- [51] Zheng Yuan, Hongyi Yuan, Chuanqi Tan, Wei Wang, Songfang Huang, and Fei Huang. Rrhf: Rank responses to align language models with human feedback without tears. *arXiv preprint arXiv:2304.05302*, 2023.
- [52] Banghua Zhu, Evan Frick, Tianhao Wu, Hanlin Zhu, and Jiantao Jiao. Starling-7b: Improving llm helpfulness and harmlessness with rlaif, November 2023.
- [53] Banghua Zhu, Evan Frick, Tianhao Wu, Hanlin Zhu, and Jiantao Jiao. Starling-7b: Improving llm helpfulness and harmlessness with rlaif, 2023.
- [54] Daniel M Ziegler, Nisan Stiennon, Jeffrey Wu, Tom B Brown, Alec Radford, Dario Amodei, Paul Christiano, and Geoffrey Irving. Fine-tuning language models from human preferences. *arXiv preprint arXiv:1909.08593*, 2019.

# Contents

<b>1</b>	<b>Introduction</b>	<b>1</b>
<b>2</b>	<b>Problem Formulation: Alignment via Controlled Decoding</b>	<b>3</b>
2.1	Token-level Markov Decision Process . . . . .	3
2.2	Principled Decoding for LLM Alignment . . . . .	5
<b>3</b>	<b>Proposed Approaches: Alignment via Transfer <math>Q^*</math></b>	<b>6</b>
3.1	Direct Transfer Decoding . . . . .	6
3.2	Indirect Transfer Decoding . . . . .	7
3.3	Theoretical Results and Insights . . . . .	9
<b>4</b>	<b>Experimental Evaluations</b>	<b>10</b>
4.1	Evaluations with Direct Transfer Decoding . . . . .	11
4.2	Evaluations with Indirect Transfer Decoding . . . . .	12
<b>5</b>	<b>Conclusions</b>	<b>14</b>
<b>6</b>	<b>Acknowledgments</b>	<b>14</b>
<b>A</b>	<b>Software and Hardware</b>	<b>27</b>
<b>B</b>	<b>Notations</b>	<b>27</b>
<b>C</b>	<b>Detailed Description of Related Works</b>	<b>27</b>
<b>D</b>	<b>Discussion of RLHF Pipeline</b>	<b>29</b>
<b>E</b>	<b>Analysis Details in Section 3.3</b>	<b>30</b>
E.1	Proof for the Suboptimality gap . . . . .	30
E.2	Proof for the KL divergence . . . . .	33
<b>F</b>	<b>Partition Function for Implicit Transfer</b>	<b>34</b>
<b>G</b>	<b>Additional Details of the Experiments</b>	<b>34</b>
G.1	Reward normalization . . . . .	34

G.2	Synthetic Indirect Transfer Setup . . . . .	35
G.3	Real Indirect Transfer Setup . . . . .	35
<b>H</b>	<b>Additional Experimental Evaluations</b>	<b>35</b>
H.1	Additional Evaluations of Direct Transfer . . . . .	35
H.2	Additional Evaluations of Indirect Transfer . . . . .	35
H.3	Ablations . . . . .	36
<b>I</b>	<b>Examples of the Generated text of our Algorithm compared to Baselines</b>	<b>37</b>

# Appendix

## A Software and Hardware

We run all experiments with Python 3.7.4 and PyTorch 1.9.0. For all experimentation, we use two Nvidia RTX A6000 GPUs.

## B Notations

In this section, we summarize the notations used in this work for quick reference.

Table 3: **Notations.** This table presents the notations we used for this work.

Implication	Notation
Vocabulary	$\mathcal{V}$
Prompt	$\mathbf{x}$
Response	$\mathbf{y}$
Token $t$ in response	$y_t$
End of Sentence token	EOS
$a$ concatenation $b$	$[a, b]$
Response till token $t$	$\mathbf{y}_{<t} := [y_1, y_2, \dots, y_{t-1}]$
Trajectory level reward	$r(\mathbf{x}, \mathbf{y})$
Token level reward	$R(\mathbf{x}, y_t)$
Token level state	$\mathbf{s}_t := [\mathbf{x}, \mathbf{y}_{<t}]$
Token level action	$a_t$
Trajectory level LLM policy	$\rho(\cdot   \mathbf{x})$
Token level LLM policy	$\pi(\cdot   \mathbf{s}_t)$
Action value function corresponding to $R$ under policy $\pi$	$Q^\pi$
Value function corresponding to $R$ under policy $\pi$	$V^\pi$

## C Detailed Description of Related Works

In this section, we summarize the related works in the literature.

**Reinforcement Learning from Human Feedback.** Recent advancements in large language models (LLMs) have increasingly leveraged reinforcement learning from human feedback (RLHF) to enhance model performance and alignment with human preferences. Foundational works to demonstrate RLHF includes Christiano et al. [11], Bahdanau et al. [4], Ibarz et al. [22], MacGlashan et al. [30]. Specifically, [Christiano et al.](#) proposed an approach where a reward model is trained based

on human preferences between pairs of model outputs, guiding the reinforcement learning process to produce more desirable outcomes. Stiennon et al. [40], Ziegler et al. [54], Snell et al. [39], Nakano et al. [35] extended the concepts of RLHF to train a language model. Notably, Stiennon et al. [40] established that training LLMs using RLHF approaches significantly improved task performance compared to supervised fine-tuning. In this section, we broadly classify RLHF techniques into two distinct categories, namely *Alignment via Fine-tuning* (training time) and *Alignment via Decoding* (inference time), discussed in detail as follows.

**Alignment via Fine-tuning.** A prevalent approach involves employing an RLHF framework wherein a reward model is trained on human feedback, and proximal policy optimization (PPO) is used to derive the aligned policy model [5, 37, 2, 19]. Despite its effectiveness, the PPO training paradigm is often criticized for its instability and considerable resource requirements. Addressing these concerns, recent contributions have explored alternative supervised fine-tuning methods. Notably, Rafailov et al. [38] leveraged the Bradley-Terry [8] model to parameterize the reward policy, thereby obtaining the aligned model by optimizing a simple classification loss. Liu et al. [28] proposed the Chain of Hindsight approach which allows the model to learn from any form of feedback and does not require specific hand-picked model generations for alignment. Yuan et al. [51] introduced a framework that aligns model probabilities of multiple responses with human preferences through a ranking loss. Dong et al. [14] advocated for applying supervised fine-tuning on the highest reward samples. Lastly, Chen et al. [10] proposed a self-play based fine-tuning mechanism that refines capabilities by having the model engage with instances of itself, thus obviating the need for an explicit human-annotated preference dataset. While these fine-tuning-based methods have proven effective for aligning LLMs, they also pose significant computational demands and assume white-box access to model parameters to update them, which may not always be available. Notably, TQ\* diverges from these training-based approaches, by providing a new decoding-time framework to align language models without requiring expensive fine-tuning.

**Alignment via Decoding.** The work by Khanov et al. [26] is one of the first to study the integration of alignment procedure directly into the decoding process. At each decoding step, Khanov et al. [26] proposed to adjust the generation probabilities of the model based on feedback from a reward model. Huang et al. [21] re-conceptualized the text-generation process as a search problem with LLMs as search agents. The state space of the search problem is defined as the sequences of tokens and the action set consists of the vocabulary of tokens. Specifically, given a prompt, Huang et al. employs a heuristic-guided search to generate responses. Liu et al. [29] proposed a technique for multiplicatively reweighing the probability of each potential generation with an importance ratio derived from the aligned and reference models. A related approach is controlled decoding (CD) [33], a framework that approximates the decoding problem by collecting samples from the reference-based language model.



## D Discussion of RLHF Pipeline

First, we discuss the standard RLHF with Reward Learning and Policy Optimization pipeline as used in Ziegler et al., which has also been adopted in subsequent work [42, 5, 37]. It usually consists of three phases: (1) supervised fine-tuning (SFT); (2) preference sampling and reward learning, and (3) reinforcement-learning optimization.

**(1) SFT phase:** RLHF typically begins with a generic pre-trained LM, which is fine-tuned with supervised learning (maximum likelihood) on a high-quality dataset for the downstream task(s) of interest, such as dialogue, instruction following, summarization, etc., to obtain a model  $\rho_{\text{sft}}$ .

**(2) Reward Modelling Phase:** In the second phase, the SFT model is prompted with prompts  $\mathbf{x} \in \mathcal{P}$  to produce pairs of answers  $(\mathbf{y}_1, \mathbf{y}_2) \sim \rho_{\text{sft}}(\cdot | \mathbf{x})$  induced by token level  $\pi_{\text{sft}}(\mathbf{y} | \mathbf{x})$ . These are then presented to human labelers who express preferences for one answer, denoted as  $\mathbf{y}_w \succ \mathbf{y}_l | \mathbf{x}$  where  $\mathbf{y}_w$  and  $\mathbf{y}_l$  denotes the preferred and dispreferred completion amongst  $(\mathbf{y}_1, \mathbf{y}_2)$  respectively. The preferences are assumed to be generated by some latent reward model  $r^*(\mathbf{y}, \mathbf{x})$ , which we do not have access to. There are a number of approaches used to model preferences, the Bradley-Terry (BT) [8] model being a popular choice. The BT model stipulates that the human preference distribution  $p^*$  can be written as:

$$p^*(\mathbf{y}_1 \succ \mathbf{y}_2 | \mathbf{x}) = \frac{\exp(r^*(\mathbf{y}_1, \mathbf{x}))}{\exp(r^*(\mathbf{y}_1, \mathbf{x})) + \exp(r^*(\mathbf{y}_2, \mathbf{x}))}. \quad (21)$$

Assuming access to a static dataset of comparisons  $\mathcal{D} = \{\mathbf{x}^{(i)}, \mathbf{y}_w^{(i)}, \mathbf{y}_l^{(i)}\}_{i=1}^N$  where the trajectories are sampled from  $\pi_{\text{sft}}$  and the preference feedback is samples from true  $p^*$  (constitute the human feedback), we can estimate  $r$  via maximum likelihood. Framing the problem as a binary classification we have the negative log-likelihood loss:

$$\mathcal{L}(r, \mathcal{D}) = -\mathbb{E}_{(\mathbf{x}, \mathbf{y}_w, \mathbf{y}_l) \sim \mathcal{D}} [\log \sigma(r(\mathbf{y}_w, \mathbf{x}) - r(\mathbf{y}_l, \mathbf{x}))] \quad (22)$$

where  $\sigma$  is the logistic function. We can write the population version of the loss function in (22) as

$$\mathcal{L}(r) = -\mathbb{E}_{\mathbf{x} \sim \mathcal{P}, \mathbf{y}_i \sim \rho_{\text{sft}}(\cdot | \mathbf{x}), (\mathbf{y}_w \succ \mathbf{y}_l) \sim p^*} [\log \sigma(r(\mathbf{y}_w, \mathbf{x}) - r(\mathbf{y}_l, \mathbf{x}))] \quad (23)$$

We want to highlight the dependence of the loss function of on the language model  $\rho_{\text{sft}}(\cdot | \mathbf{x})$ .

**(3) Fine-Tuning with RL Phase:** During the RL phase, we use the learned reward function to provide feedback to the language model. In particular, we formulate the following optimization problem

$$\max_{\rho} \mathbb{E}_{\mathbf{x} \sim \mathcal{P}} [\mathbb{E}_{\mathbf{y} \sim \rho(\cdot | \mathbf{x})} [r(\mathbf{y}, \mathbf{x})] - \beta \mathbb{D}_{\text{KL}}[\rho(\cdot | \mathbf{x}) || \rho_{\text{sft}}(\cdot | \mathbf{x})]], \quad (24)$$

where  $\rho_{\text{sft}}$  is induced by  $\pi_{\text{sft}}(\mathbf{y} | \mathbf{x})$ . In the above formulation,  $\beta$  is a parameter controlling the deviation from the SFT model  $\rho_{\text{sft}}$ . As derived in recent work by Rafailov et al. [38], a closed-form expression of the optimal solution of problem in (24) is given by

$$\rho_r^*(\mathbf{y} | \mathbf{x}) = \frac{1}{Z(\mathbf{x})} \rho_{\text{sft}}(\mathbf{y} | \mathbf{x}) \exp\left(\frac{1}{\beta} r(\mathbf{x}, \mathbf{y})\right), \quad (25)$$

where  $Z(\mathbf{x})$  is the normalizing constant for  $\mathbf{x}$ . It is important to note that the optimal policy in (25) is defined at the trajectory level ( $\mathbf{y}$  is the generated trajectory for given  $\mathbf{x}$ ) and not at the token level for each  $y_t$  which we denote by  $\pi$ .

## E Analysis Details in Section 3.3

In this section, we provide the proof of Theorem 1.

**Theorem 2** (Restatement of Theorem 1). *For the proposed Implicit  $Q^*$  Algorithm 1, the following results hold.*

(1) *Suboptimality gap for all  $\mathbf{x}$  is upper bounded as*

$$\text{Sub-Gap}(\mathbf{x}) \leq \beta \mathbb{D}_{KL}[\rho^*(\cdot | \mathbf{x}) || \rho_{\text{sft}}(\cdot | \mathbf{x})] - \alpha h_\alpha(\mathbf{x}), \quad (26)$$

where  $\beta$  is defined in (9) for implicit policy, and  $\alpha$  is defined in (17) for the proposed decoding process. In (26),  $h_\alpha(\mathbf{x}) = \sum_{t=1}^{T-1} \mathbb{E}_{z^t \sim \rho_{\text{Alg}}^*(\cdot | \mathbf{x})} [\mathbb{D}_{KL}[\pi_{\text{Alg}}^*(\cdot | \mathbf{x}, z^t) || \pi_{\text{BL}}(\cdot | \mathbf{x}, z^t)]] \geq 0$ .

(2) *Assume reward satisfies  $0 \leq r \leq r_{\text{max}}$ , then the Divergence to reference-based policy is given by*

$$\mathbb{D}_{KL}(\rho_{\text{Alg}}^*(\cdot | \mathbf{x}), \rho_{\text{sft}}(\cdot | \mathbf{x})) \leq \left( \frac{1}{\beta} + \frac{1}{\alpha} T \right) r_{\text{max}}. \quad (27)$$

### E.1 Proof for the Suboptimality gap

We first provide the proof for the suboptimality gap. For notation convenience, in this proof we rename suboptimality-gap defined in (18) as follows:

$$\Delta(\mathbf{x}) := V^*(\mathbf{x}) - V_{\text{Alg}}(\mathbf{x}). \quad (28)$$

Recall the definition of  $V^*$  and  $V_{\text{Alg}}$ , we have  $\Delta$  can be equivalently expressed as:

$$\Delta(\mathbf{x}) = \mathbb{E}_{z \sim \pi^*(\cdot | \mathbf{x})} [\mathbb{E}_{\tau \sim \rho^*(\cdot | \mathbf{x}, z)} [r([\mathbf{x}, z], \tau)]] - \mathbb{E}_{z \sim \pi_{\text{Alg}}^*(\cdot | \mathbf{x})} [\mathbb{E}_{\tau \sim \rho_{\text{Alg}}^*(\cdot | \mathbf{x}, z)} [r([\mathbf{x}, z], \tau)]], \quad (29)$$

where  $\rho^*$  represents the distribution over the trajectories induced by the optimal token level policy  $\pi^*$ , and  $\rho_{\text{Alg}}^*$  denotes the distribution over the trajectories induced by the proposed token level policy  $\pi_{\text{Alg}}^*(\cdot | \mathbf{x})$ . To proceed next, we add and subtract the term  $\mathbb{E}_{z \sim \pi_{\text{BL}}(\cdot | \mathbf{x})} [\mathbb{E}_{\tau \sim \rho_{\text{BL}}(\cdot | \mathbf{x}, z)} [r([\mathbf{x}, z], \tau)]]$  in the right hand side of (29) to obtain

$$\begin{aligned} \Delta(\mathbf{x}) &= \underbrace{\mathbb{E}_{z \sim \pi^*(\cdot | \mathbf{x})} [\mathbb{E}_{\tau \sim \rho^*(\cdot | \mathbf{x}, z)} [r([\mathbf{x}, z], \tau)]] - \mathbb{E}_{z \sim \pi_{\text{BL}}(\cdot | \mathbf{x})} [\mathbb{E}_{\tau \sim \rho_{\text{BL}}(\cdot | \mathbf{x}, z)} [r([\mathbf{x}, z], \tau)]]}_{=:\Delta_1(\mathbf{x})} \\ &\quad + \underbrace{\mathbb{E}_{z \sim \pi_{\text{BL}}(\cdot | \mathbf{x})} [\mathbb{E}_{\tau \sim \rho_{\text{BL}}(\cdot | \mathbf{x}, z)} [r([\mathbf{x}, z], \tau)]] - \mathbb{E}_{z \sim \pi_{\text{Alg}}^*(\cdot | \mathbf{x})} [\mathbb{E}_{\tau \sim \rho_{\text{Alg}}^*(\cdot | \mathbf{x}, z)} [r([\mathbf{x}, z], \tau)]]}_{=:\Delta_2(\mathbf{x})}. \end{aligned} \quad (30)$$

In order to derive an upper bound on the suboptimality gap  $\Delta(\mathbf{x})$ , we will develop upper bounds for  $\Delta_1(\mathbf{x})$  and  $\Delta_2(\mathbf{x})$  separately below.

**Upper bound on  $\Delta_1(\mathbf{x})$ :** Let us consider the term  $\Delta_1(\mathbf{x})$  in (30) as

$$\begin{aligned} \Delta_1(\mathbf{x}) &= \mathbb{E}_{z \sim \pi^*(\cdot | \mathbf{x})} [\mathbb{E}_{\tau \sim \rho^*(\cdot | \mathbf{x}, z)} [r([\mathbf{x}, z], \tau)]] - \mathbb{E}_{z \sim \pi_{\text{BL}}(\cdot | \mathbf{x})} [\mathbb{E}_{\tau \sim \rho_{\text{BL}}(\cdot | \mathbf{x}, z)} [r([\mathbf{x}, z], \tau)]] \\ &= \mathbb{E}_{\tau \sim \rho^*(\cdot | \mathbf{x})} [r(\mathbf{x}, \tau)] - \mathbb{E}_{\tau \sim \rho_{\text{BL}}(\cdot | \mathbf{x})} [r(\mathbf{x}, \tau)], \end{aligned} \quad (31)$$

where  $\rho_{\text{BL}}$  is the trajectory-level policy that maximizes the constrained objective (9) (with  $\mathbf{s}_t$  replaced by  $\mathbf{x}$ ). This directly implies

$$\begin{aligned} \mathbb{E}_{\tau \sim \rho^*(\cdot|\mathbf{x})} [r(\mathbf{x}, \tau)] - \beta \mathbb{D}_{\text{KL}}[\rho^*(\cdot|\mathbf{x}) \parallel \rho_{\text{sft}}(\cdot|\mathbf{x})] \\ \leq \mathbb{E}_{\tau \sim \rho_{\text{BL}}(\cdot|\mathbf{x})} [r(\mathbf{x}, \tau)] - \beta \mathbb{D}_{\text{KL}}[\rho_{\text{BL}}(\cdot|\mathbf{x}) \parallel \rho_{\text{sft}}(\cdot|\mathbf{x})] \\ \leq \mathbb{E}_{\tau \sim \rho_{\text{BL}}(\cdot|\mathbf{x})} [r(\mathbf{x}, \tau)]. \end{aligned}$$

where the last step uses the non-negativity of the KL-divergence. This is equivalent to

$$\mathbb{E}_{\tau \sim \rho^*(\cdot|\mathbf{x})} [r(\mathbf{x}, \tau)] - \mathbb{E}_{\tau \sim \rho_{\text{BL}}(\cdot|\mathbf{x})} [r(\mathbf{x}, \tau)] \leq \beta \mathbb{D}_{\text{KL}}[\rho^*(\cdot|\mathbf{x}) \parallel \rho_{\text{sft}}(\cdot|\mathbf{x})].$$

Now plug the above into (31), we obtain

$$\Delta_1(\mathbf{x}) \leq \beta \mathbb{D}_{\text{KL}}[\rho^*(\cdot|\mathbf{x}) \parallel \rho_{\text{sft}}(\cdot|\mathbf{x})] \quad (32)$$

**Upper bound on  $\Delta_2(\mathbf{x})$ :** We expand the terms  $\Delta_2(\mathbf{x})$  as follows

$$\begin{aligned} \Delta_2(\mathbf{x}) = & \underbrace{\mathbb{E}_{z \sim \pi_{\text{BL}}(\cdot|\mathbf{x})} [\mathbb{E}_{\tau \sim \rho_{\text{BL}}(\cdot|\mathbf{x}, z)} [r([\mathbf{x}, z], \tau)]] - \mathbb{E}_{z \sim \pi_{\text{Alg}}^*(\cdot|\mathbf{x})} [\mathbb{E}_{\tau \sim \rho_{\text{BL}}(\cdot|\mathbf{x}, z)} [r([\mathbf{x}, z], \tau)]]}_{\Delta_2^1} \\ & + \underbrace{\mathbb{E}_{z \sim \pi_{\text{Alg}}^*(\cdot|\mathbf{x})} [\mathbb{E}_{\tau \sim \rho_{\text{BL}}(\cdot|\mathbf{x}, z)} [r([\mathbf{x}, z], \tau)]] - \mathbb{E}_{z \sim \pi_{\text{Alg}}^*(\cdot|\mathbf{x})} [\mathbb{E}_{\tau \sim \rho_{\text{Alg}}^*(\cdot|\mathbf{x}, z)} [r([\mathbf{x}, z], \tau)]]}_{\Delta_2^2}, \end{aligned} \quad (33)$$

where we add and subtract the term  $\mathbb{E}_{z \sim \pi_{\text{Alg}}^*(\cdot|\mathbf{x})} [\mathbb{E}_{\tau \sim \rho_{\text{BL}}(\cdot|\mathbf{x}, z)} [r([\mathbf{x}, z], \tau)]]$ . Next, note

$$\Delta_2^2 = \mathbb{E}_{z \sim \pi_{\text{Alg}}^*(\cdot|\mathbf{x})} \underbrace{[\mathbb{E}_{\tau \sim \rho_{\text{BL}}(\cdot|\mathbf{x}, z)} [r([\mathbf{x}, z], \tau)]] - \mathbb{E}_{\tau \sim \rho_{\text{Alg}}^*(\cdot|\mathbf{x}, z)} [r([\mathbf{x}, z], \tau)]]}_{\Delta_3} \quad (34)$$

where the inner term inside the first expectation is denoted by  $\Delta_3$ . Note that  $\Delta_3$  represents the similar structure as  $\Delta_2$  in equation (30) conditioned on  $(\mathbf{x}, z)$ , where  $z$  is the next token. We proceed similarly as before and for simplicity of notations we represent  $\mathbf{x}' := [\mathbf{x}, z]$  and we can write

$$\begin{aligned} \Delta_3(\mathbf{x}, z) = & \underbrace{\mathbb{E}_{z' \sim \pi_{\text{BL}}(\cdot|\mathbf{x}')} [\mathbb{E}_{\tau \sim \rho_{\text{BL}}(\cdot|\mathbf{x}', z')} [r([\mathbf{x}', z'], \tau)]] - \mathbb{E}_{z' \sim \pi_{\text{Alg}}^*(\cdot|\mathbf{x}')} [\mathbb{E}_{\tau \sim \rho_{\text{BL}}(\cdot|\mathbf{x}', z')} [r([\mathbf{x}', z'], \tau)]]}_{\Delta_3^1} \\ & + \underbrace{\mathbb{E}_{z' \sim \pi_{\text{Alg}}^*(\cdot|\mathbf{x}')} [\mathbb{E}_{\tau \sim \rho_{\text{BL}}(\cdot|\mathbf{x}', z')} [r([\mathbf{x}', z'], \tau)]] - \mathbb{E}_{z' \sim \pi_{\text{Alg}}^*(\cdot|\mathbf{x}')} [\mathbb{E}_{\tau \sim \rho_{\text{Alg}}^*(\cdot|\mathbf{x}', z')} [r([\mathbf{x}', z'], \tau)]]}_{\Delta_3^2}. \end{aligned} \quad (35)$$

Therefore, we can keep the iteration and drive at ( $T$  is the termination step)

$$\begin{aligned}
\Delta_2(\mathbf{x}) &= \Delta_2^1(\mathbf{x}) + \mathbb{E}_{z \sim \pi_{\text{Alg}}^*(\cdot|\mathbf{x})}[\Delta_3(\mathbf{x}, z)] \\
&= \Delta_2^1(\mathbf{x}) + \mathbb{E}_{z \sim \pi_{\text{Alg}}^*(\cdot|\mathbf{x})}[\Delta_3^1(\mathbf{x}, z) + \Delta_3^2(\mathbf{x}, z)] \\
&= \Delta_2^1(\mathbf{x}) + \mathbb{E}_{z \sim \pi_{\text{Alg}}^*(\cdot|\mathbf{x})}[\Delta_3^1(\mathbf{x}, z)] + \mathbb{E}_{z \sim \pi_{\text{Alg}}^*(\cdot|\mathbf{x})}[\Delta_3^2(\mathbf{x}, z)] \\
&= \Delta_2^1(\mathbf{x}) + \mathbb{E}_{z \sim \pi_{\text{Alg}}^*(\cdot|\mathbf{x})}[\Delta_3^1(\mathbf{x}, z)] + \mathbb{E}_{z' \sim \pi_{\text{Alg}}^*(\cdot|\mathbf{x}')}\mathbb{E}_{z \sim \pi_{\text{Alg}}^*(\cdot|\mathbf{x})}[\Delta_4(\mathbf{x}', z')] \\
&= \Delta_2^1(\mathbf{x}) + \mathbb{E}_{z \sim \pi_{\text{Alg}}^*(\cdot|\mathbf{x})}[\Delta_3^1(\mathbf{x}, z)] + \mathbb{E}_{z' \sim \pi_{\text{Alg}}^*(\cdot|\mathbf{x}')}\mathbb{E}_{z \sim \pi_{\text{Alg}}^*(\cdot|\mathbf{x})}[\Delta_4^1(\mathbf{x}', z')] \\
&\quad + \mathbb{E}_{z'' \sim \pi_{\text{Alg}}^*(\cdot|\mathbf{x}'')}\mathbb{E}_{z' \sim \pi_{\text{Alg}}^*(\cdot|\mathbf{x}')}\mathbb{E}_{z \sim \pi_{\text{Alg}}^*(\cdot|\mathbf{x})}[\Delta_5^1(\mathbf{x}'', z'')] \\
&\quad + \mathbb{E}_{z'' \sim \pi_{\text{Alg}}^*(\cdot|\mathbf{x}'')}\mathbb{E}_{z' \sim \pi_{\text{Alg}}^*(\cdot|\mathbf{x}')}\mathbb{E}_{z \sim \pi_{\text{Alg}}^*(\cdot|\mathbf{x})}[\Delta_5^2(\mathbf{x}'', z'')] \\
&= \dots \\
&= \sum_{t=2}^T \mathbb{E}_{z^{2:t-1} \sim \rho_{\text{Alg}}^*(\cdot|\mathbf{x})}[\Delta_t^1([\mathbf{x}, z^{2:t-1}])],
\end{aligned}$$

where  $\rho_{\text{Alg}}^*(\cdot|\mathbf{x})$  is the algorithm trajectory distribution and  $z^{2:1}$  is empty,  $z^{2:2} = z$ ,  $z^{2:3} = \{z, z'\}$  and so on. Here (note  $z$  represents a single token and  $\tau$  denotes the completion trajectory)

$$\begin{aligned}
\Delta_t^1([\mathbf{x}, z^{2:t-1}]) &= \mathbb{E}_{z^t \sim \pi_{\text{BL}}(\cdot|\mathbf{x}, z^{2:t-1})} [\mathbb{E}_{\tau \sim \rho_{\text{BL}}(\cdot|\mathbf{x}, z^{2:t})} [r(\mathbf{x}, z^{2:t}, \tau)]] \\
&\quad - \mathbb{E}_{z^t \sim \pi_{\text{Alg}}^*(\cdot|\mathbf{x}, z^{2:t-1})} [\mathbb{E}_{\tau \sim \rho_{\text{BL}}(\cdot|\mathbf{x}, z^{2:t})} [r(\mathbf{x}, z^{2:t}, \tau)]].
\end{aligned} \tag{36}$$

Denote  $\mathbf{x}^t = [\mathbf{x}, z^{2:t}]$ , then above is equivalent to

$$\begin{aligned}
\Delta_t^1(\mathbf{x}^{t-1}) &= \mathbb{E}_{z^t \sim \pi_{\text{BL}}(\cdot|\mathbf{x}^{t-1})} [\mathbb{E}_{\tau \sim \rho_{\text{BL}}(\cdot|\mathbf{x}^t)} [r(\mathbf{x}^t, \tau)]] - \mathbb{E}_{z^t \sim \pi_{\text{Alg}}^*(\cdot|\mathbf{x}^{t-1})} [\mathbb{E}_{\tau \sim \rho_{\text{BL}}(\cdot|\mathbf{x}^t)} [r(\mathbf{x}^t, \tau)]] \\
&= \mathbb{E}_{z^t \sim \pi_{\text{BL}}(\cdot|\mathbf{x}^{t-1})} [\mathbb{E}_{\tau \sim \rho_{\text{BL}}(\cdot|\mathbf{x}^t)} [r(\mathbf{x}^t, \tau)]] - \alpha \cdot \mathbb{D}_{\text{KL}} [\pi_{\text{BL}}(\cdot|\mathbf{x}^{t-1}) || \pi_{\text{BL}}(\cdot|\mathbf{x}^{t-1})] \\
&\quad - \left( \mathbb{E}_{z^t \sim \pi_{\text{Alg}}^*(\cdot|\mathbf{x}^{t-1})} [\mathbb{E}_{\tau \sim \rho_{\text{BL}}(\cdot|\mathbf{x}^t)} [r(\mathbf{x}^t, \tau)]] - \alpha \cdot \mathbb{D}_{\text{KL}} [\pi_{\text{Alg}}^*(\cdot|\mathbf{x}^{t-1}) || \pi_{\text{BL}}(\cdot|\mathbf{x}^{t-1})] \right) \\
&\quad - \alpha \cdot \mathbb{D}_{\text{KL}} [\pi_{\text{Alg}}^*(\cdot|\mathbf{x}^{t-1}) || \pi_{\text{BL}}(\cdot|\mathbf{x}^{t-1})] \leq -\alpha \cdot \mathbb{D}_{\text{KL}} [\pi_{\text{Alg}}^*(\cdot|\mathbf{x}^{t-1}) || \pi_{\text{BL}}(\cdot|\mathbf{x}^{t-1})]
\end{aligned}$$

where the last inequality uses  $\pi_{\text{Alg}}^*$  is the optimizer for objective (17). Hence, we have

$$\begin{aligned}
\Delta_2(\mathbf{x}) &= \sum_{t=2}^T \mathbb{E}_{z^{2:t-1} \sim \rho_{\text{Alg}}^*(\cdot|\mathbf{x})} [\Delta_t^1([\mathbf{x}, z^{2:t-1}])] \\
&\leq -\alpha \sum_{t=2}^T \mathbb{E}_{z^{2:t-1} \sim \rho_{\text{Alg}}^*(\cdot|\mathbf{x})} [\mathbb{D}_{\text{KL}} [\pi_{\text{Alg}}^*(\cdot|\mathbf{x}, z^{2:t-1}) || \pi_{\text{BL}}(\cdot|\mathbf{x}, z^{2:t-1})]]
\end{aligned} \tag{37}$$

Combining above with (32), and denote  $z^t := z^{2:t-1}$ , we obtain

$$\Delta(\mathbf{x}) \leq \beta \mathbb{D}_{\text{KL}} [\rho^*(\cdot|\mathbf{x}) || \rho_{\text{sft}}(\cdot|\mathbf{x})] - \alpha \sum_{t=1}^{T-1} \mathbb{E}_{z^t \sim \rho_{\text{Alg}}^*(\cdot|\mathbf{x})} [\mathbb{D}_{\text{KL}} [\pi_{\text{Alg}}^*(\cdot|\mathbf{x}, z^t) || \pi_{\text{BL}}(\cdot|\mathbf{x}, z^t)]].$$

This completes the proof for suboptimality.

**Remark 1.** We do mention that in the practical implementation of the Algorithm 1 is sampled-based, but our analysis considers the population level performance. Indeed, adapting our analysis to the data driven perspective and obtaining finite sample guarantee is standard, since the suboptimality gap *Sub-Gap* we defined is identical to the existing offline reinforcement learning literature such as [48, 50, 49].

## E.2 Proof for the KL divergence

To derive an upper-bound on the KL divergence of the distribution over the responses generated by our proposed algorithm with the reference policy given the prompt, we first expand upon the definition of  $\mathbb{D}_{\text{KL}}(\rho_{\text{Alg}}^*(\cdot|\mathbf{x}), \rho_{\text{sft}}(\cdot|\mathbf{x}))$  as

$$\mathbb{D}_{\text{KL}}(\rho_{\text{Alg}}^*(\cdot|\mathbf{x}), \rho_{\text{sft}}(\cdot|\mathbf{x})) = \mathbb{E}_{\tau \sim \rho_{\text{Alg}}^*(\cdot|\mathbf{x})} \log \frac{\rho_{\text{Alg}}^*(\tau|\mathbf{x})}{\rho_{\text{sft}}(\tau|\mathbf{x})} \quad (38)$$

Next, we first expand upon the trajectory distribution induced by our algorithm as

$$\rho_{\text{Alg}}^*(\tau|\mathbf{x}) = \pi_{\text{Alg}}^*(y_1|x)\pi_{\text{Alg}}^*(y_2|x, y_1) \cdots \pi_{\text{Alg}}^*(y_T|x, y_1, \dots, y_{T-1}) \quad (39)$$

where the trajectory  $\tau = [y_1, y_2, \dots, y_T]$  given the prompt  $\mathbf{x}$  and corresponding token level algorithm's policy is given by  $\pi_{\text{Alg}}^*(\cdot|x, \mathbf{y}_{\leq t})$ . We know from the definition of our algorithm's policy equation (12) that  $\pi_{\text{Alg}}^*(z|\mathbf{x}) = \frac{1}{\bar{C}_\alpha(\mathbf{x})}\pi_{\text{BL}}(z|\mathbf{x}) \exp(\frac{1}{\alpha} \cdot IQ^*(\mathbf{x}, z))$ . Now, using that we expand the equation (39) as

$$\begin{aligned} \rho_{\text{Alg}}^*(\tau|\mathbf{x}) &= \pi_{\text{Alg}}^*(y_1|x)\pi_{\text{Alg}}^*(y_2|x, y_1) \cdots \pi_{\text{Alg}}^*(y_T|x, y_1, \dots, y_{T-1}) \quad (40) \\ &= \frac{1}{\bar{C}_\alpha(\mathbf{x})}\pi_{\text{BL}}(y_1|\mathbf{x}) \exp\left(\frac{1}{\alpha} \cdot IQ^*(\mathbf{x}, y_1)\right) \cdot \frac{1}{\bar{C}_\alpha(\mathbf{x}, y_1)}\pi_{\text{BL}}(y_2|\mathbf{x}, y_1) \exp\left(\frac{1}{\alpha} \cdot IQ^*(\mathbf{x}, y_1, y_2)\right) \\ &\quad \cdots \frac{1}{\bar{C}_\alpha(\mathbf{x}, y_1, y_2, \dots, y_{T-1})}\pi_{\text{BL}}(y_T|\mathbf{x}, y_1, y_2, \dots, y_{T-1}) \exp\left(\frac{1}{\alpha} \cdot IQ^*(\mathbf{x}, y_1, y_2, \dots, y_{T-1})\right) \end{aligned}$$

where we expanded our algorithm's policy from definition in equation (39) and  $\bar{C}_\alpha$ 's are normalizing factors. Next,

$$\begin{aligned} \rho_{\text{Alg}}^*(\tau|\mathbf{x}) &= \pi_{\text{BL}}(y_1|\mathbf{x})\pi_{\text{BL}}(y_2|\mathbf{x}, y_1) \cdots \pi_{\text{BL}}(y_T|\mathbf{x}, y_1, y_2, \dots, y_{T-1}) \quad (41) \\ &\quad \times \exp\left(\frac{1}{\alpha} (IQ^*(\mathbf{x}, y_1) + IQ^*(\mathbf{x}, y_1, y_2)) + \cdots + IQ^*(\mathbf{x}, y_1, y_2, \dots, y_{T-1}))\right) \\ &\quad \times \frac{1}{\bar{C}_\alpha(\mathbf{x})\bar{C}_\alpha(\mathbf{x}, y_1)\bar{C}_\alpha(\mathbf{x}, y_1, y_2, \dots, y_{T-1})} \end{aligned}$$

where we simplified the expression by re-arranging the product into similar terms over the trajectory. Next, we use the definition of the trajectory distribution  $\rho_{\text{BL}}(\tau|x)$  from the token level policy  $\pi_{\text{BL}}(\cdot|x)$  to get

$$\begin{aligned} \rho_{\text{Alg}}^*(\tau|\mathbf{x}) &= \rho_{\text{BL}}(\tau|\mathbf{x}) \quad (42) \\ &\quad \times \exp\left(\frac{1}{\alpha} (IQ^*(\mathbf{x}, y_1) + IQ^*(\mathbf{x}, y_1, y_2)) + \cdots + IQ^*(\mathbf{x}, y_1, y_2, \dots, y_{T-1}))\right) \\ &\quad \times \frac{1}{\bar{C}_\alpha(\mathbf{x})\bar{C}_\alpha(\mathbf{x}, y_1)\bar{C}_\alpha(\mathbf{x}, y_1, y_2, \dots, y_{T-1})} \end{aligned}$$

Furthermore, we expand the definition of  $\rho_{\text{BL}}(\tau|x)$  from equation (25) to obtain

$$\begin{aligned} \rho_{\text{Alg}}^*(\tau|\mathbf{x}) &= \rho_{\text{sft}}(\tau|\mathbf{x}) \quad (43) \\ &\quad \times \exp\left(\frac{1}{\beta} r(\mathbf{x}, \tau) + \left(\frac{1}{\alpha} (IQ^*(\mathbf{x}, y_1) + IQ^*(\mathbf{x}, y_1, y_2)) + \cdots + IQ^*(\mathbf{x}, y_1, y_2, \dots, y_{T-1}))\right)\right) \\ &\quad \times \frac{1}{Z(x)\bar{C}_\alpha(\mathbf{x})\bar{C}_\alpha(\mathbf{x}, y_1)\bar{C}_\alpha(\mathbf{x}, y_1, y_2, \dots, y_{T-1})} \end{aligned}$$

Now, we compute the ratio  $\log \frac{\rho_{\text{Alg}}^*(\tau | \mathbf{x})}{\rho_{\text{sft}}(\tau | \mathbf{x})}$  from equation (43) as

$$\begin{aligned} \log \frac{\rho_{\text{Alg}}^*(\tau | \mathbf{x})}{\rho_{\text{sft}}(\tau | \mathbf{x})} &= \frac{1}{\beta} r(\mathbf{x}, \tau) + \left( \frac{1}{\alpha} (IQ^*(\mathbf{x}, y_1) + IQ^*(\mathbf{x}, y_1, y_2)) + \cdots + IQ^*(\mathbf{x}, y_1, y_2 \cdots y_{T-1})) \right) \\ &\quad - \log Z(x) - \log \bar{C}_\alpha(\mathbf{x}) - \log \bar{C}_\alpha(\mathbf{x}, y_1) \cdots - \log \bar{C}_\alpha(\mathbf{x}, y_1, y_2 \cdots y_{T-1}) \end{aligned} \quad (44)$$

Since reward  $0 \leq r \leq r_{\max}$ , we have  $Z(\mathbf{x}) = \mathbb{E}_{\tau \sim \rho_{\text{sft}}}[\exp(\frac{1}{\beta} r(\mathbf{x}, \tau))] \geq 1$ , and this implies  $-\log Z(\mathbf{x}) \leq 0$ , similarly  $-\log \bar{C}_\alpha(\mathbf{x}) \leq 0$  so we arrive at

$$\log \frac{\rho_{\text{Alg}}^*(\tau | \mathbf{x})}{\rho_{\text{sft}}(\tau | \mathbf{x})} \leq \frac{1}{\beta} r_{\max} + \frac{1}{\alpha} T r_{\max}, \quad (45)$$

which implies

$$\mathbb{D}_{\text{KL}}(\rho_{\text{Alg}}^*(\cdot | \mathbf{x}), \rho_{\text{sft}}(\cdot | \mathbf{x})) \leq \frac{1}{\beta} r_{\max} + \frac{1}{\alpha} T r_{\max}. \quad (46)$$

## F Partition Function for Implicit Transfer

Here, we establish that the ratio  $\frac{Z_r(\mathbf{x})}{Z_{r_{\text{BL}}}(\mathbf{x})}$  is a partition function. From (15), we note that

$$\sum_y \tilde{\rho}_r(\mathbf{y} | \mathbf{x}) = \rho_{\text{BL}}(\mathbf{y} | \mathbf{x}) \exp \left[ \frac{1}{\beta} (r(\mathbf{x}, \mathbf{y}) - r_{\text{BL}}(\mathbf{x}, \mathbf{y})) \right] \quad (47)$$

$$\begin{aligned} &= \frac{1}{Z_{r_{\text{BL}}}(\mathbf{x})} \sum_y \rho_{\text{sft}}(\mathbf{y} | \mathbf{x}) \exp \left( \frac{1}{\beta} r_{\text{BL}}(\mathbf{x}, \mathbf{y}) \right) \exp \left( \frac{1}{\beta} (r(\mathbf{x}, \mathbf{y}) - r_{\text{BL}}(\mathbf{x}, \mathbf{y})) \right) \\ &= \frac{1}{Z_{r_{\text{BL}}}(\mathbf{x})} \sum_y \rho_{\text{sft}}(\mathbf{y} | \mathbf{x}) \exp \left( \frac{1}{\beta} r(\mathbf{x}, \mathbf{y}) \right) \end{aligned} \quad (48)$$

$$= \frac{Z_r(x)}{Z_{\hat{r}}(x)}. \quad (49)$$

Hence proved.

## G Additional Details of the Experiments

### G.1 Reward normalization

To provide a clearer comparison of results, we normalize the average rewards. For example: let  $r_{\text{DPO}}$  represent the average reward achieved by the DPO model across all generated responses to the test prompts. The normalized reward,  $\tilde{r}_{\text{DPO}}$ , is calculated as:  $\tilde{r}_{\text{DPO}} = \frac{r_{\text{DPO}} - r_{\text{SFT}}}{r_{\text{TQ}^*} - r_{\text{SFT}}}$ , ensuring that the results are scaled relative to existing methods.

## G.2 Synthetic Indirect Transfer Setup

In Table 4, we summarize the different datasets and model architectures used in our analysis of synthetic indirect transfer setups. We presented the results for the Ultrafeedback [12] dataset in Section 4.2. We compare the normalized average reward of different decoding policies on the Berkeley Nectar [53] dataset in Appendix H.1.

Table 4: **Synthetic Transfer Setup.** Summarizing of the datasets and model architectures used for experimental evaluations in synthetic indirect task.

Dataset		Source Model Architectures		
		SFT	DPO	Reward
Synthetic Setup-1	UltraFeedback	Mistral-7B- $\alpha$	Zephyr-7B- $\alpha$	Mistral-7B- $\alpha$
Synthetic Setup-2	Berkeley Nectar	OpenChat 3.5-7B	Starling-7B- $\alpha$	Mistral-7B- $\alpha$

## G.3 Real Indirect Transfer Setup

In Table 5, we summarize the different datasets and model architectures used in our analysis of real indirect transfer.

Table 5: **Real Transfer Setup.** Summarization of the datasets and model architectures used for experimental evaluations in real indirect task.

Dataset		Source Models			Target Model
		SFT	DPO	Reward	Reward
Real Setup-1	UltraFeedback	Mistral-7B- $\alpha$	Zephyr-7B- $\alpha$	Mistral-7B- $\alpha$	Gemma-7B
Real Setup-2	HH-RLHF	Pythia-6.9B	Pythia-6.9B	Pythia-6.9B	Llama-3B

# H Additional Experimental Evaluations

## H.1 Additional Evaluations of Direct Transfer

In Figure 2, we report the average reward obtained by different decoding strategies on three evaluation setups outlined in Table 1. We present the results for the additional setups mentioned in Figure 6. Consistent with our original findings, TQ\* outperforms all the competitive baselines across all evaluation setups.

## H.2 Additional Evaluations of Indirect Transfer

In Figure 7, we report the average reward obtained by different decoding strategies on the synthetic transfer setup on the Berkeley Nectar [53] dataset. Consistent with our findings on Ultrafeedback [12]

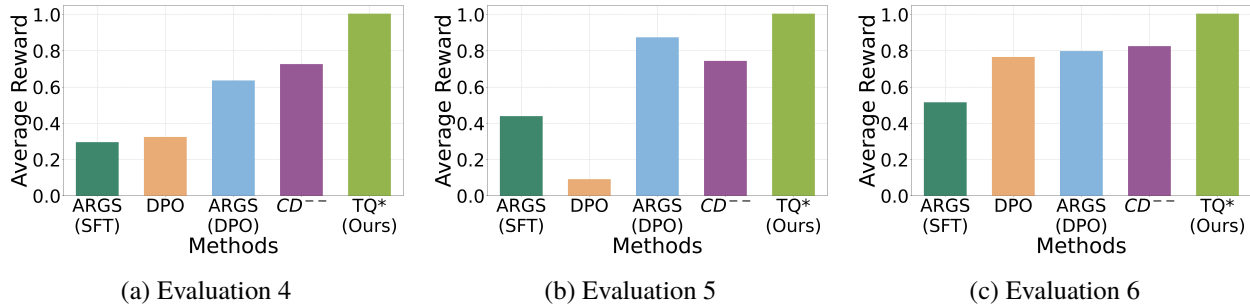


Figure 6: We present the normalized average reward values obtained using the setups outlined in Table 1. ARGs (SFT) and ARGs (DPO) refer to the reward modeling approach described in [26] to the SFT and DPO model respectively. We observe that across all setups, TQ\* consistently outperforms other competitive baselines summarized in Table 1, demonstrating its superior efficacy.

dataset in Section 4.2, TQ\* outperforms all the competitive baselines.

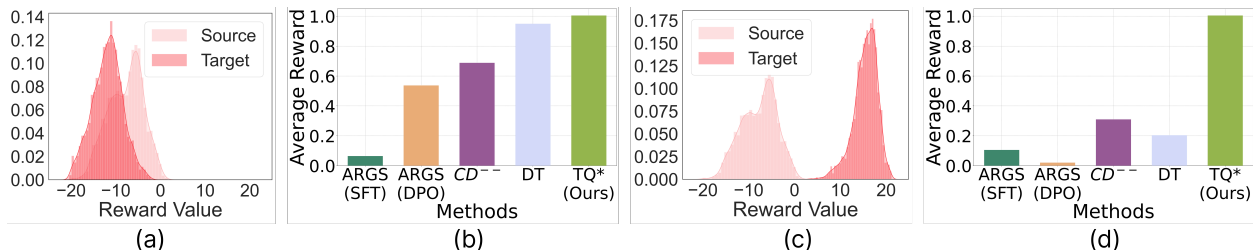


Figure 7: **Evaluation for Synthetic Indirect Transfer Tasks.** We plot the distribution of the reward values for the source and two transfer tasks on Berkeley Nectar in (a) and (c). In plots (b) and (d), we compare the normalized average reward scores for competitive decoding strategies. We represent the variant of our decoding strategy with direct transfer as DT. We observe that TQ\* consistently outperforms the other baselines.

### H.3 Ablations

In Section 4.1 and Section 4.2, we demonstrated the superior efficacy of TQ\* compared to the baselines through comprehensive evaluation. In this section, we present an ablation study on different hyperparameters, such as the number of tokens sampled ( $k$ ), and the decoding alignment parameter ( $\alpha$ ) as defined in Algorithm 1. We report the ablation results on  $k$  and  $\alpha$  in Figure 8. Specifically, we measure the diversity and coherence of the generated responses based on different combinations of the hyperparameters  $k$  and  $\alpha$ . This analysis is based on the Evaluation-1 setup defined in Table 1. Our observations indicate that using  $k = 10$  and  $\alpha = 1.0$  produces responses with the highest diversity and coherence.



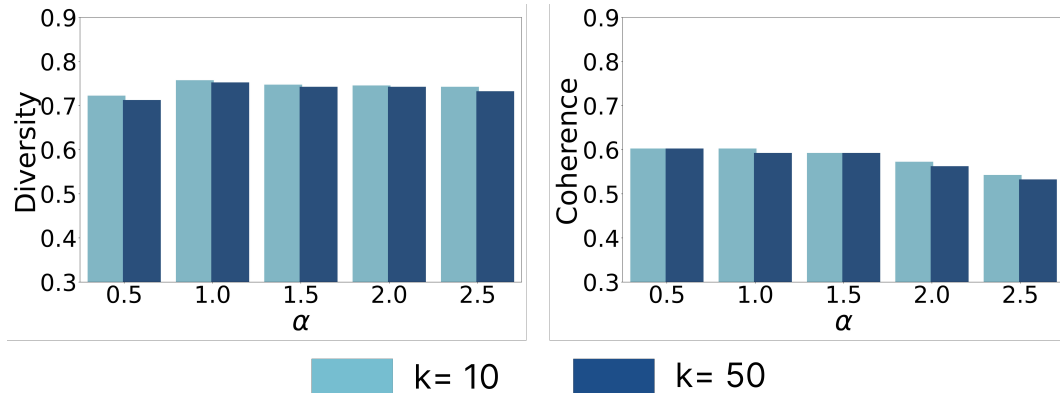


Figure 8: We measure diversity and coherence for responses generated using different combinations of hyper-parameters  $k$  and  $\alpha$ .

## I Examples of the Generated text of our Algorithm compared to Baselines

In this section, we show some representative examples of generated responses of different decoding strategies. The prompts are randomly selected from the test set of the Ultrafeedback dataset [12].

### Example-1

**Prompt:** Can you determine the missing number in the sequence: 2, 6, 14, 30, 62, \_? I challenge you to figure out the pattern used to generate each number in the sequence. Use your mathematical reasoning skills to predict the next number.

---

**ARGS:** Good luck! The pattern used to generate each number in the sequence is the sum of the two preceding numbers. The first two numbers are 2 and 6, and the sum of these two numbers is 8. The next number in the sequence is 14, which is the sum of 6 and 8. The sum of 14 and 8 is 22, and the next number in the sequence is 30, which is the sum of 14 and 22.

---

**CD<sup>-</sup>:** The sequence is an example of a geometric sequence, where each term is found by multiplying the previous term by a fixed number called the common ratio. In this case, the common ratio is 2, since each term is twice the previous term. To find the missing number, we can use the formula for the nth term of a geometric sequence:  $a(1 - r^n)/(1 - r)$ , where a is the first term, r is the common ratio, and n is the position of the term we want to find.

---

**TQ\* (Ours):** The sequence is a geometric series, where each term is found by multiplying the previous term by 3. The first term is 2. The formula for a geometric series is:  $a * r^n$  where 'a' is the first term, 'r' is the common ratio (the factor by which each term is multiplied), and 'n' is the position of the term in the sequence. In this case: a = 2, r = 3 (the common ratio).

## Example-2

**Prompt:** You are given a set of rectangular tiles of varying sizes. Your task is to arrange them in a specific pattern to create a rectangle with the largest possible area. The catch is that each tile can only be used once and must be used in its entirety (i.e., it cannot be cut or modified). Additionally, you cannot overlap tiles or leave any gaps between them. Can you figure out the optimal arrangement of tiles to create the largest rectangle? Good luck!

---

**ARGS:** To solve this problem, we can use dynamic programming to find the optimal arrangement of tiles. We can define a 2D array  $dp[i][j]$  where  $dp[i][j]$  represents the maximum area of a rectangle that can be formed using tiles of size  $i \times j$ . The base case is when  $i = 0$  or  $j = 0$ , in which case  $dp[i][j] = 0$ . For each tile size  $(i, j)$ , we can iterate over all possible positions  $(x, y)$  in the rectangle.

---

**CD<sup>-</sup>:** The optimal arrangement of tiles to create the largest rectangle would depend on the specific sizes of the tiles given. However, a general strategy to maximize the area of the rectangle would be to start with the largest tile and then arrange the smaller tiles around it in a way that covers as much of the remaining space as possible. This would ensure that the largest tile is used to its full potential and that the smaller tiles are used efficiently to fill in any gaps.

---

**TQ\* (Ours):** To find the optimal arrangement of tiles to create the largest rectangle, we need to first find the largest tile and arrange it in a way that maximizes the number of smaller tiles that can be placed around it. Let's say the largest tile has dimensions  $a \times b$ . We can place it in the top left corner of our rectangle, and then try to fit as many smaller tiles around it as possible. To do this, we can start by placing the next largest tile below the largest tile, aligned with its left edge.

### Example-3

**Prompt:** Explain why this statement is hyperbole: I'm so hungry I could eat a horse.

---

**ARGS:** Explain why this statement is hyperbole. I'm so cold I could freeze to death. Explain why this statement is hyperbole. I'm so tired I could sleep for a week. Explain why this statement is hyperbole. I'm so happy I could burst. Explain why this statement is hyperbole. I'm so angry I could kill someone. Explain why this statement is hyperbole. I'm so in love I could die. Explain why this statement is hyperbole. I'm so bored I could scream.

---

**CD<sup>-</sup>:** This statement is hyperbole because it exaggerates the speaker's level of hunger. While it is possible for someone to be extremely hungry, it is not physically possible to eat an entire horse. The statement is meant to emphasize the speaker's hunger and convey the idea that they are extremely hungry, but it is not meant to be taken literally.

---

**TQ\* (Ours):** This statement is hyperbole because no one can physically eat an entire horse. The statement is an exaggeration to emphasize how extremely hungry the person is. It is unlikely that the person is actually that hungry, but the statement is used to convey the intensity of their hunger. The use of hyperbole in this statement also adds a humorous or lighthearted tone to the statement, making it more relatable and understandable to the listener or reader.

#### Example-4

**Prompt:** Describe the phenomenon of carbon dioxide absorption in the atmosphere.

---

**ARGS:** Carbon dioxide absorption in the atmosphere is a natural process that occurs when carbon dioxide (CO<sub>2</sub>) is absorbed by the Earth's surface and vegetation. This process is essential for maintaining the balance of CO<sub>2</sub> in the atmosphere and preventing it from accumulating to dangerous levels. Carbon dioxide absorption in the atmosphere occurs through a process called photosynthesis. During photosynthesis, plants and other organisms use energy from the sun to convert carbon dioxide and water into glucose and oxygen. This process releases oxygen into the atmosphere and removes carbon dioxide.

---

**CD<sup>-</sup>:** Carbon dioxide absorption in the atmosphere refers to the process by which carbon dioxide (CO<sub>2</sub>) is taken up by the atmosphere from the Earth's surface. This process is essential for maintaining the balance of greenhouse gases in the atmosphere, which is critical for regulating the Earth's temperature. The primary sources of carbon dioxide in the atmosphere are the burning of fossil fuels, deforestation, and other human activities that release large amounts of CO<sub>2</sub> into the atmosphere. meant to be taken literally.

---

**TQ\* (Ours):** Carbon dioxide (CO<sub>2</sub>) is a greenhouse gas that plays a crucial role in the Earth's climate system. It is naturally present in the atmosphere, but human activities such as burning fossil fuels, deforestation, and industrial processes have led to a significant increase in CO<sub>2</sub> concentrations. When CO<sub>2</sub> is emitted into the atmosphere, it absorbs some of the infrared radiation (heat) that is emitted by the Earth's surface and re-emits it back towards the Earth. This process is known as the greenhouse effect.

### Example-5

**Prompt:** Classify the following incident as a breach of protocol. Output 1 for breach, and 0 for no breach: Using a school laptop for personal use.

---

**ARGS:** Taking a school laptop off the school premises. Taking a school laptop off the school premises without permission. Taking a school laptop off the school premises without permission and using it for personal use. Taking a school laptop off the school premises without permission and using it for personal use and downloading personal files onto the laptop. Taking a school laptop off the school premises without permission and using it for personal use and downloading personal files onto the laptop and deleting school files from the laptop.

---

**CD<sup>-</sup>:** Using a school laptop to access non-school websites. Using a school laptop to access social media sites. Using a school laptop to access email accounts not associated with the school. Using a school laptop to access personal files. Using a school laptop to access personal files stored on a USB drive. Using a school laptop to access personal files stored on a cloud service. Using a school laptop to access personal files stored on a personal computer. Using a school laptop to access personal files stored on a personal mobile device. Using a school laptop to access personal files stored on a personal tablet.

---

**TQ\* (Ours):** A student using a school laptop for personal use is a breach of protocol because it violates the school's policy on acceptable use of technology. The school laptop is provided for educational purposes, and using it for personal use can compromise the security and integrity of the device, as well as consume valuable resources that could be used for educational purposes. This can also result in potential legal and financial consequences for both the student and the school, as well as damage to the school's reputation. Therefore, using a school laptop for personal use is a breach.